Draft version December 1, 2016
Preprint typeset using LaTeX style emulateapj v. 01/23/15

Two Peculiar Fast Transients in a Strongly Lensed Host Galaxy

S. A. Rodney[1,] and The FrontierSN Team

Draft version December 1, 2016

ABSTRACT

Two unusual transient events were observed by the Hubble Space Telescope in 2014, appearing in a galaxy at z=1.0054±0.0002 that is gravitationally lensed by the galaxy cluster MACS J0416.1-2403. These transients—collectively nicknamed "Spock"— were faster and fainter than any supernova, but significantly more luminous than a classical nova: they reached peak luminosities of $\sim 10^{41}$ erg s^{-1} in $\lesssim$5 rest-frame days, then faded below detectability in roughly the same timespan. Lens models of the foreground cluster suggest that it is entirely plausible that the two events are *spatially* coincident at the source plane, but very unlikely that they were also *temporally* coincident. We find that *Spock* can plausibly be classified as a recurrent nova, a luminous blue variable, or a stellar caustic crossing event—but all three explanations require either an extreme astrophysical source or highly unusual gravitational lensing.

1. INTRODUCTION

The Spock transient events—separately designated HFF14Spo-1 and HFF14Spo-2—appeared in Hubble Space Telescope (*HST*) imaging collected in January and August of 2014, respectively (Figure 1). These images were centered on the galaxy cluster MACS J0416.1-2403 (hereafter, MACS0416) and were collected as part of the Hubble Frontier Fields (HFF) survey (HST-PID:13496, PI:Lotz), a multi-cycle program for deep imaging of 6 massive galaxy clusters and associated "blank sky" fields observed in parallel.

Combining the *HST* imaging and lens models of the MACS0416 gravitational lens leads to three key observables for the HFF14Spo events: (1) they are both more luminous than a classical nova, but less luminous than almost all supernovae (SNe), reaching a peak luminosity of roughly 10^{41} erg s^1 ($M_V = 14$); (2) both transients exhibited fast light curves, with rise and decline timescales of $\sim 2 - -5$ days in the rest frame; and (3) it is likely that both events arose from the same physical location but were not coincident in time—they were probably separated by 3-5 months in the rest frame. These peculiar transients thus present an intriguing puzzle: they are broadly consistent with the expected behavior of stellar explosions (they each exhibit a single isolated rise and decline in brightness), but they can not be trivially classified into any of the common categories of explosive or eruptive astrophysical transients.

The HFF survey was not designed with discovery of peculiar extragalactic transients as a core objective, but it has unintentionally opened an unusual window of discovery for such events. Very faint sources at relatively high redshift in these fields are made detectable by the substantial gravitational lensing magnification of the foreground galaxy clusters. Very rapidly evolving sources are also more likely to be found, due to the necessity of a rapid cadence for repeat imaging in the HFF program. These unusual characteristics for an *HST* survey contributed to the early detection and characterization of SN Refsdal, the first SN that is strongly lensed into multiple resolved images (Kelly *et al.* 2015). The HFF imaging program has also enabled a precise measurement of the lensing magnification for SN Tomas, a high-redshift Type Ia SN (Rodney *et al.* 2015). Both of those SNe constitute fairly common astrophysical phenomena, and the possibility of discovering such transients was anticipated at the start of the HFF program. HFF14Spo, however, appears to be *sui generis*. No single astrophysical model is clearly sufficient to explain all of the available observational data, and the best available models require either an extreme stellar source or a very unusual gravitational lensing configuration.

[1] Department of Physics and Astronomy, University of South Carolina, 712 Main St., Columbia, SC 29208, USA
srodney@sc.edu

2. RESULTS

The two HFF14Spo events exhibited very similar light curves, as shown in Figures 2. The January event, HFF14Spo-1, rose to peak luminosity and faded back to quiescence in only ∼7 days, and the August event, HFF14Spo-2, rose and fell in $<$ 20 days. The host galaxy for both HFF14Spo events is at a redshift of $z = 1.0054 \pm 0.0002$ (see Methods section 6). After dividing the observed rise/fall timescales by $(1 + z)$ to correct for cosmic time dilation, we see that both events exhibited a charactierstic timescale of ∼2–5 days in the rest frame.

To interpret the observed light curves and the timing of these two events, we use five independently constructed cluster mass models to determine the effects of gravitational lensing from the MACS J0416.1-2403 cluster. As reported in Table 1, these lens models predict absolute magnification values between about $\mu = 10$ and $\mu = 100$ for both events. This wide range is due primarily to the close proximity of the HFF14Spo events to the lensing critical curve for sources at $z = 1$. Note that the magnifications for HFF14Spo-1 and HFF14Spo-2 are highly correlated. A variation of a given lens model that moves the critical curve closer to the position of HFF14Spo-1 would drive the magnification of that event much higher (toward $\mu_1 \sim 100$), but that would also have the effect of moving the critical curve farther from HFF14Spo-2 which would necessarily drive its magnification down-

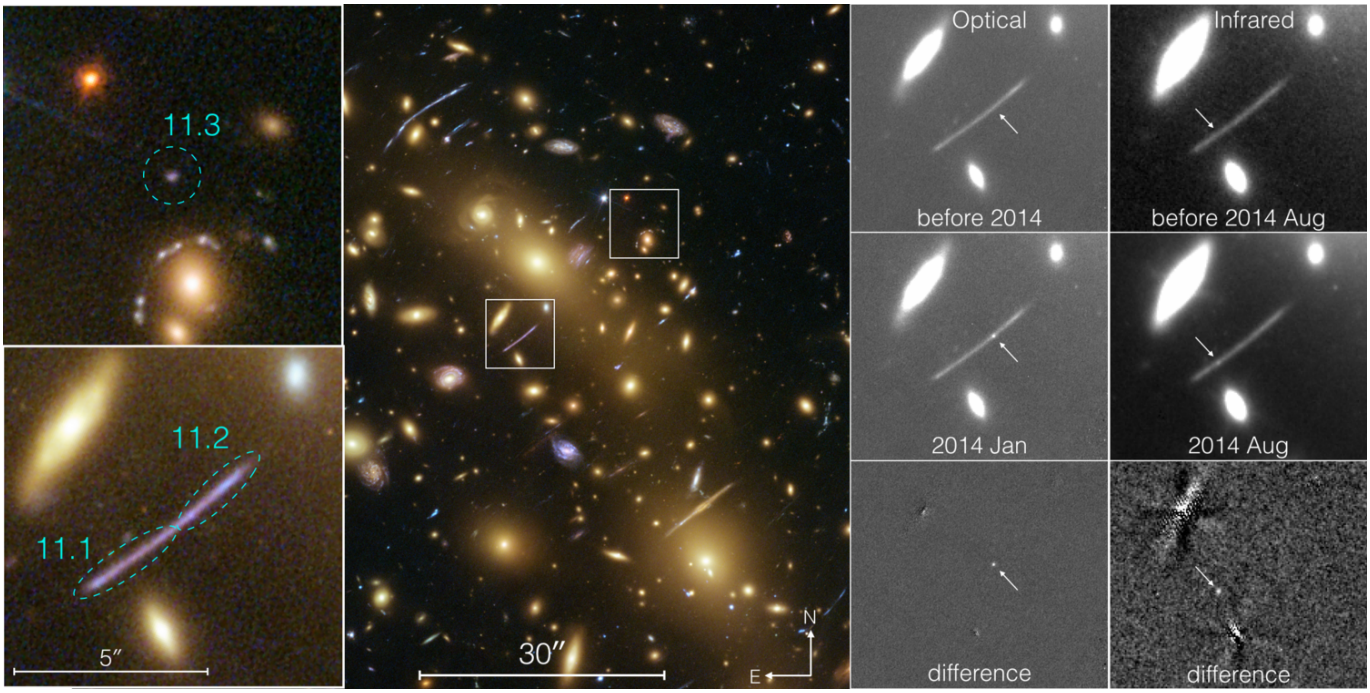

FIG. 1.— The detection of HFF14Spo-1 and HFF14Spo-2 in HST imaging from the Hubble Frontier Fields. The central panel shows the full field of the MACSJ0416 cluster, in a combined image using optical and infrared bands from HST. Two boxes within the main panel demarcate the regions where the HFF14Spo host galaxy images appear. These regions are shown as two inset panels on the left, highlighting the three images of the host galaxy (labeled 11.1, 11.2, and 11.3), whcih are caused by the gravitational lensing of the cluster. Two columns on the right side show the discovery of the two transient events in optical and infrared light, respectively. In these final two columns the top row is a template image, the center row shows the epoch when each transient appeared, and the bottom row is the difference image.

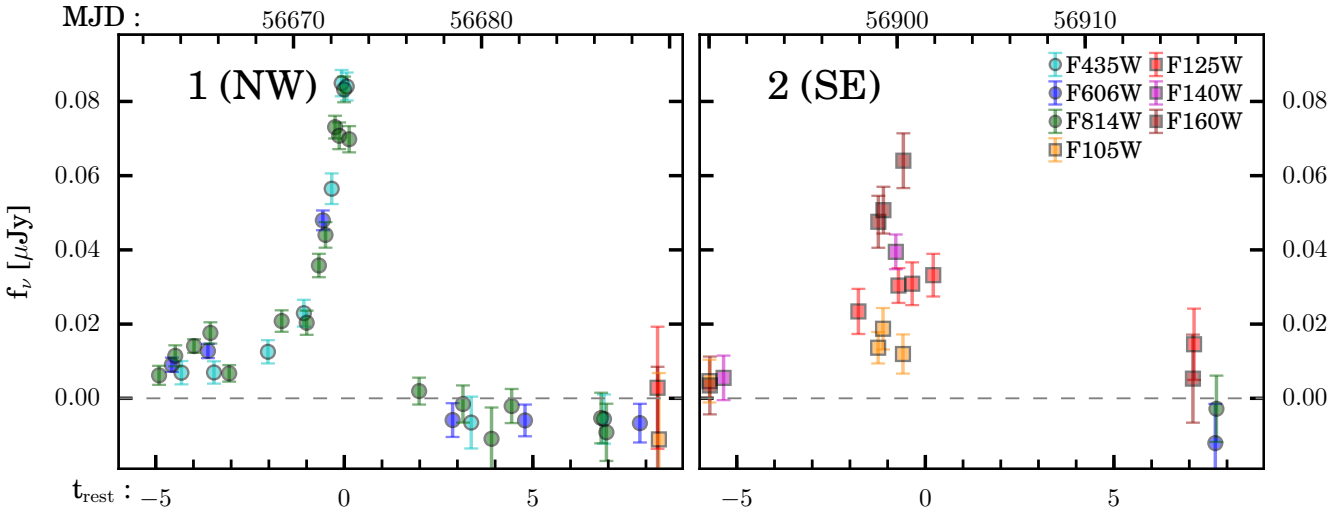

FIG. 2.— Light curves for the two transient events, HFF14Spo-1 on the left and HFF14Spo-2 on the right. Measured fluxes in micro-Janskys are plotted against rest-frame time at $z = 1.0054$, relative to the time of the peak observed flux for each event. The corresponding Mean Julian Date (MJD) in the observer frame is marked on the top axis for each panel. As indicated in the legend, optical observations using the *HST* ACS-WFC detector are plotted as circles in shades of blue and green, while infrared measurements from the WFC3-IR detector are plotted as red, orange and purple squares.

TABLE 1
Lens model predictions for time delays and magnifications.

Model	$\Delta t_{\rm NW:SE}$ (days)	$\Delta t_{\rm NW:11.3}$ (years)	μ_1	μ_2	μ_3
Bradac	42^{+13}_{-9}	-3.7 ±0.3	90^{+61}_{-27}	32^{+8}_{-10}	$3.6^{+0.2}_{-0.5}$
Bradac-v3	···	···	38 ±8	12.8 ±0.8	2.9 ±0.1
Diego	-48±10	0.8	35±20	30±20	
Jauzac-A	29 ±3	-2.2 ±0.1	36^{+4}_{-3}	17 ±1	4.5 ±0.1
Jauzac-B	28^{+5}_{-7}	$-2.2^{+0.1}_{-0.2}$	37 ±3	18 ±2	4.6 ±0.1
Jauzac-C	$2.5^{+0.8}_{-1.0}$	-3.0 ±0.1	37^{+4}_{-3}	16^{+1}_{-2}	3.2 ±0.05
Kawamata	$4.1^{+5.5}_{-3.4}$	$-5.0^{+0.5}_{-0.6}$	29^{+43}_{-10}	84^{+103}_{-38}	$3.0^{+0.2}_{-0.2}$
Williams	-10^{+1}_{-7}	$-2.5^{+1.0}_{-3.1}$	13^{+11}_{-6}	12^{+9}_{-5}	$3.1^{+2.2}_{-0.9}$
Zitrin	42^{+13}_{-9}	-3.7 ±0.3	90^{+61}_{-27}	32^{+8}_{-10}	$3.6^{+0.2}_{-0.5}$

Note. — Each lens model is identified by the last name of the lead modeler or the principal investigator of the modeling team. Time delays give the predicted delay relative to an appearance in the NW host image, 11.2. Positive (negative) values indicate the NW image is the leading (trailing) image of the pair.

ward (toward $\mu_2 \sim 10$).

From each model we also extract two time delay predictions, given in Table 1. We report all time delays relative to the HFF14Spo-1 event, which appeared in January 2014 in host image 11.2.

Most optical transient events observed in extragalactic surveys can be explained as stellar explosions of one type or another. As the HFF14Spo transients do not easily match the most common stellar explosive events (e.g., novae and SNe), a useful starting point for classification is to examine the phase space of peak luminosity versus decline time (see, e.g., Kasliwal *et al.* 2010). To infer the luminosity and decline time for each HFF14Spo event, we combine the linear fits to the light curves (shown in Figure 4) with the predicted range of lensing magnifications (Figure 9. For any assumed value for the time of peak brightness, the light curve fits give us an estimate of the "observed" peak magnitude and a corresponding rise-time and decline-time measurement. We then convert this extrapolated peak magnitude to a luminosity (e.g., νL_ν in erg s^{-1}) by first correcting for the luminosity distance assuming a standard ΛCDM cosmology, and then accounting for an assumed lensing magnification, μ. At the end of all this, we have a grid of possible peak luminosities for each event as a function of magnification and time of peak (or, equivalently, the decline time).

Figure 3 shows the resulting constraints on the peak luminosity and the decline time, which we quantify as t_2, the time over which the transient declines by 2 magnitudes. Shaded green and red bands represent the HFF14Spo-1 and HFF14Spo-2 events, respectively, and in each case they incorporate the allowed range for time of peak (see Figure 4) and the lensing magnification ($10 < \mu < 100$) as reported in Table 1. The two events are largely consistent with each other, and if both events are representative of a single system (or a homogeneous class) then the most likely peak luminosity and decline time (the region with the most overlap) would be $L_{\rm pk} \sim 10^{41}$ ergs/s and $t_3 \sim 1.8$ days.

The colored regions along the right side of Figure **??** mark the luminosity and decline times for SNe and SN-like transients. This includes the familiar luminosity-decline relation of Type Ia SNe (Phillips 1993) and the broad heterogeneous class of Core Collapse SNe, as well as less well-understood classes such as Superluminous SNe (Gal-Yam 2012; Arcavi *et al.* 2016), Type Iax SNe (Foley *et al.* 2013), fast optical transients (Drout *et al.* 2014), Ca-rich SNe (Filippenko *et al.* 2003; Perets *et al.* 2011; Kasliwal *et al.* 2012), and Luminous Red Novae (also called intermediate luminosity red transients; Munari *et al.* 2002; Kulkarni *et al.* 2007; Kasliwal *et al.* 2011a). The HFF14Spo events are incompatible with all of these explosion categories, owing to the very rapid rise and fall of both HFF14Spo light curves, and their relatively low peak luminosities of $\sim 10^{41}$ erg s^{-1}.

Dashed boxes in Figure **??** represent categories of "SN-like" stellar explosions that have been theoretically predicted and extensively modeled, but for which very few viable candidates have actually been observed. Both of these categories come closer to matching the observed characteristics of the two HFF14Spo events, so they warrant closer scrutiny.

The dashed rectangle in Figure **??** represents the "kilonova" class (also called a "macronova" or "mini-supernova"), which is a theorized category of optical transient that may be generated by the merger of a neutron star (NS) binary. Such a NS+NS merger can drive a relativistic jet that may be observed as a Gamma Ray Burst (GRB) and would emit gravitational waves. These may also be accompanied by a very rapid optical light curve (the kilonova component) that is driven by the radioactive decay of r-process elements in the ejecta (Li and Paczyński 1998; Kulkarni 2005). To date there are two cases of fast optical transients associated with GRB events, which have been interpreted as possible kilonovae (Perley *et al.* 2009; Tanvir *et al.* 2013). The HFF14Spo transients fall within the range of theoretically predicted peak luminosity and decline times for kilonovae. However, the rise time for the HFF14Spo-1 event is at least 5 days in the rest-frame, which is significantly longer than the < 1 day rise expected for a kilonova (e.g. Metzger *et al.* 2010; Barnes and Kasen 2013; Kasen *et al.* 2015). Furthermore, both HFF14Spo events are either significantly fainter or faster than the optical light curves for the two existing kilonova candidates.

The dashed oval in Figure **??** represents the ".Ia" class of He shell explosions (Bildsten *et al.* 2007). These are theorized to arise from AM Canum Venaticorum (AM CVn) systems, which are binary star systems transferring He onto a C/O or O/Ne WD primary (Warner 1995; Nelemans and Tout 2005). Bildsten *et al.* (2007) argued that these systems can build up enough He on the surface of the WD to trigger a thermonuclear runaway and possibly a detonation. A typical AM CVn system could produce ∼10 He shell flashes over $\sim 10^6$ yr, while the He mass transfer rate is slow enough to admit thermally unstable burning in the WD's accreted He shell. The final He shell flash is the brightest, and is what we refer to as the .Ia event. This last explosion may or may not lead to a detonation of the WD core (the double detonation scenario; Nomoto 1982a,b; Woosley and Weaver 1986, 1994).

Theoretical .Ia models suggest that the light curves

would be quite bright, reaching a peak luminosity of $\sim 10^{42}$ erg s^{-1}. That is comparable to the brightness of a normal SN, but the .Ia light curves would decline much more quickly. After an initial short peak (3-5 days) driven by the rapid radioactive decay of ^{48}Cr and ^{52}Fe at the exterior of the ejecta, a secondary decline phase kicks in, powered by the slower ^{56}Ni decay chain (Shen *et al.* 2010). The optical emission is expected to fade by 2 magnitudes after $\sim$ 10 days. There have been a few viable .Ia candidates presented in the literature (Kasliwal *et al.* 2010; Perets *et al.* 2010; Poznanski *et al.* 2010), but we do not have enough objects to empirically constrain .Ia light curve shapes. Although the HFF14Spo light curves were somewhat fainter and faster than the expectations for a .Ia event, there is enough uncertainty about the diversity of .Ia light curves that this model should not be dismissed on those merits alone.

2.0.1. *The Recurrence Problem*

An additional challenge for applying any SN-like transient model to explain the HFF14Spo events is the problem of the apparent recurrence. For all of these catastrophic stellar explosions we do not expect to see repeated transient events: the kilonova progenitor system is completely destroyed by the merger, and for the .Ia explosions the principal observed transient event is the last transient episode that system produces. Even if we suppose that an AM CVn system could produce repeated He shell flashes of similar luminosity, the period of recurrence would be of order 10^5 yr, making these effectively non-recurrent sources.

Thus, the only way to reconcile these cataclysmic explosion models with the two observed HFF14Spo events is to either (a) assert that the two events are two images of the same explosion, appearing to us separately only because of a gravitational lensing time delay (as was the case for the 5 images of SN Refsdal Kelly *et al.* 2015, 2016), or (b) invoke a highly serendipitous occurrence of two unrelated peculiar explosions in the same host galaxy in the same year.

To evaluate scenario (a), in which a lensing time delay causes the appearance of two separate events, we must rely on the available lens modeling. We have seen in Section 9 that none of the MACS J0416.1-2403 lens models predict an 8 month time delay between appearances in image 11.1 and 11.2. This is represented in Figure 8, where we have plotted the light curves for the two transient events, along with shaded vertical bars marking the time delay predictions of all models. To accept this time-delayed single explosion explanation for HFF14Spo, we would have to assume that a large systematic bias is similarly affecting all of the lens models. While we cannot rule out such a bias, the consistency of the lens modeling makes this scenario less tenable.

For the latter scenario of two unrelated explosions, it is difficult to assess the likelihood of such an occurrence quantitatively, as there are no measured rates of .Ia or kilonovae. In a study of very fast optical transients with the Pan-STARRS1 survey, Berger *et al.* (2013) derived a limit of $\lesssim 0.05$ Mpc^{-3} yr^{-1} for transients reaching $M \approx -14$ mag on a timescale of $\sim$1 day. This limit, though several orders of magnitude higher than the constraints on novae or SNe, is sufficient to make it exceedingly unlikely that two such transients would appear in the same galaxy in a single year. Furthermore, we have observed no other transients with similar luminosities and light curve shapes in our high-cadence surveys of 5 other Frontier Fields clusters. Indeed, all other transients detected in the core Frontier Fields survey have been fully consistent with normal SNe. Thus, we have no evidence to suggest that transients of this kind are much more common at $z \sim 1$.

2.1. *Luminous Blue Variable*

The transient sources categorized as Luminous Blue Variables (LBVs) are the result of eruptions or explosive episodes from massive stars ($> 10 M_\odot$). The class is exemplified by well-studied examples such as P Cygni and η Carinae (η Car) in the Milky Way and S Doradus (S-Dor) in the Large Magellanic Cloud (for recent overviews of the LBV class, see Smith *et al.* 2011; Kochanek *et al.* 2012). Although the association with massive stars is well established, this class is very heterogeneous and there is currently a vigorous debate over the precise nature of the progenitor pathway (Smith and Tombleson 2015; Humphreys *et al.* 2016; Smith 2016). The "Great Eruptions" of such massive stars are sometimes labeled as "SN impostors" because these most prominent transient episodes can exhibit light curves reminiscent of core collapse SNe, reaching peak absolute magnitudes of $\sim$-7 to -16 mag in optical bands, and lasting for tens to hundreds of days. In some cases the LBV progenitor does indeed culminate with a final true core collapse SN event (Mauerhan *et al.* 2013; Tartaglia *et al.* 2016, e.g.)

Although most giant LBV eruptions have been observed to last much longer than the HFF14Spo events (Smith *et al.* 2011), some LBVs have exhibited repeated rapid outbursts that are broadly consistent with the very fast HFF14Spo light curves. Because of this commonly seen stochastic variability, the LBV scenario does not have any trouble accounting for the HFF14Spo events as two separate episodes.

Two well-studied LBVs in particular provide a plausible match to the observed HFF14Spo events. The first is the transient "SN 2009ip" (Maza *et al.* 2009) which was later re-classified as an LBV as it showed repeated brief transient episodes (e.g., Miller *et al.* 2009; Li *et al.* 2009; Berger *et al.* 2009; Drake *et al.* 2010). Pre-eruption HST imaging demonstrated that the progenitor of SN 2009ip was likely a very high mass star ($\gtrsim 50$ M$_\odot$, Smith *et al.* 2010; Foley *et al.* 2011). Remarkably, this star eventually did explode as a true SN event, observed in 2012 (Mauerhan *et al.* 2013; Pastorello *et al.* 2013; Prieto *et al.* 2013).

The second useful comparison object is NGC3432-LBV1 (also called SN 2000ch), which was first observed as a bright variable star (Papenkova and Li 2000) and later definitively classified as an LBV (Wagner *et al.* 2004). This event exhibited at least three significant outbursts over 2-year period, which were observed in a concerted monitoring campaign (Pastorello *et al.* 2010). The spectral characteristics of this LBV suggest a similarity to Wolf-Rayet stars (Pastorello *et al.* 2010) and the variation of the SED suggests modulated dusty wind (Wagner *et al.* 2004; Kochanek *et al.* 2012). The observed sequence of erratic transient episodes may also be indicative of binary interactions similar to S-Dor (Pastorello *et al.* 2010; Smith *et al.* 2011).

Figure 11 presents a direct comparison of the observed HFF14Spo light curves against the light curves of these two rapid-eruption LBVs, SN 2009ip and NGC3432-LBV1. The brief outbursts of these LBVs have been less finely sampled than the two HFF14Spo events, but the available data show a wide variety of rise and decline times, even for a single object over a relatively narrow time window of a few months. For each of the rapid LBV outbursts shown in Figure 11 we have measured the peak luminosity and the decline time, allowing these events to be plotted in the $L_{\rm pk}$ vs. t_2 space of Figure 3 (as orange diamonds). All of the rapid LBV eruptions of SN 2009ip and NGC3432-LBV1 provide only upper limits on t_2, due to the relatively sparse photometric sampling. The observations of both HFF14Spo events are consistent with the observed luminosities and decline times of the fastest and brightest of rapid LBV outbursts.

In addition to the relatively short and very bright giant eruptions shown in Figure 11, most LBVs also commonly exhibit a slower underlying variability that has not been observed at the HFF14Spo locations. P Cygni and η Car, for example, slowly rose and fell in brightness by $\sim$1 to 2 mag over a timespan of several years before and after their historic giant eruptions. Such variation has not been detected at the HFF14Spo locations, as can be seen from the wide views of the HFF14Spo light curves in Figure 8. Nevertheless, given the broad range of light curve behaviors seen in LBV events, we can not reject this class as a possible explanation for the HFF14Spo system.

TODO: Measure this more quantitatively: forced photometry in drz (not diff) images at all epochs, estimate what would be the magnitude of a quiescent eta-Car-like star, and would we be able to detect a 1-2 mag brightening over the span of the HFF campaign

2.1.1. *Physical Implications of the LBV Model*

Considering the population of LBVs, the observed HFF14Spo events would stand out as extreme events. The observed rise and decline times for HFF14Spo would place both among the most rapid LBV eruptions ever seen. The peak luminosities of both HFF14Spo-1 and HFF14Spo-2 are similar to the observed luminosities of rapid, bright outbursts seen in LBVs such as SN 2009ip and NGC3432-LBV1. However, the upper edge of the range of plausible peak luminosities for both HFF14Spo events reaches 10^{42} erg s^{-1}, which would be an order of magnitude more luminous than any rapid outburst from those two nearby LBVs.

The precise physical mechanism for LBV outbursts is still not fully understood. LBV stars such as η Carshow clear evidence of ejected shells of gas, and very massive stars are known to undergo extensive mass loss as they evolve toward eventual explosion as a SN. This has led to the canonical model of LBV transient events as being the optical signature of an eruptive mass loss episode. Such mass loss could arise from a variety of direct mechanisms, such as continuum-driven super-Eddington winds (Smith and Owocki 2006), pulsational pair instability ejections (Woosley *et al.* 2007), and shock heating of stellar envelopes from internal shell-burning instabilities (Dessart *et al.* 2010). This is far from an exhaustive list, and none of these explanations are entirely sufficient to account for all of the observed diversity of LBV behaviors or the structural complexity the most well-studied LBVs (e.g. Smith *et al.* 2011; Kochanek *et al.* 2012).

Although we do not have a complete physical model in hand, we can nevertheless explore some of the physical implications of an LBV classification for the two HFF14Spo events. We first make a rough estimate of the total radiated energy, which can be computed using the decline timescale t_2 and the peak luminosity $L_{\rm pk}$ following Smith *et al.* (2011):

$$E_{\rm rad} = \zeta t_2 L_{\rm pk}, \quad (1)$$

where ζ is a factor of order unity that depends on the precise shape of the light curve.[2] Adopting $L_{\rm pk} \sim 10^{41}$ erg s^{-1} and $t_2 \sim$2 days (as shown in Figure 3), we find that the total radiated energy isi $E_{\rm rad} \sim 10^{46}$ erg. A realistic range for this estimate would span $10^{44} < E_{\rm rad} < 10^{47}$ erg, due to uncertainties in the magnification, bolometric luminosity correction, decline time, and light curve shape (in roughly that order of importance). These uncertainties notwithstanding, our crude estimate does fall well within the range of plausible values for the total radiated energy of a major LBV outburst.

If LBV eruptions are driven by significant mass ejection events, then the energy budget would also include a substantial amount of kinetic energy imparted to the ejected gas shell. Without spectroscopic information from the HFF14Spo transients we can not place any realistic estimate on the kinetic energy. Nevertheless, we can take the radiated energy as a rough lower limit on the total energy release and ask what timescale would be required for a massive star to build up that amount of energy. This approach assumes that the energy released in an LBV eruption is generated slowly in the stellar interior and is in some way "bottled up" by the stellar envelope, before being released in a rapid mass ejection. The "build-up" timescale to match the radiative energy release is then

$$t_{\rm rad} = \frac{E_{\rm rad}}{L_{\rm qui}} = t_2 \frac{\xi L_{\rm pk}}{L_{\rm qui}}, \quad (2)$$

where $L_{\rm qui}$ is the luminosity of the LBV progenitor star during quiescence. For the HFF14Spo events we have no useful constraint on the quiescent luminosity, but for evaluating the LBV scenario we can assume it is similar to the local LBVs whose progenitors have been directly observed. This gives a range for the radiative build-up timescale between $t_{\rm rad} \sim$ 30 days if the progenitor is η Car-like ($M_V \sim -12$), or $t_{\rm rad} \sim$ 20 years if it is similar to the faintest known LBV progenitors (e.g. SN 2010dn, with $M_V \sim -6$).

Alternatively, a more informative approach is to assert that the build-up timescale for HFF14Spo corresponds to the observed rest-frame lag between the two events, roughly 120 days. Adopting $L_{\rm pk} = 10^{41}$ erg s^{-1} and $t_2 =$ 2 days, if we assume $t_{\rm rad} =$ 120 days we can infer that the quiescent luminosity of the HFF14Spo progenitor would be $L_{\rm qui} \sim 10^{39.5}$ erg s-1 ($M_V \sim -10$). This is a very reasonable quiescent luminosity value for the massive ($>$ 10M$_\odot$) progenitor stars expected for LBVs.

Although the above discussion shows that the observations of the HFF14Spo transients are largely consis-

[2] Note that Smith *et al.* (2011) used $t_{1.5}$ instead of t_2, which amounts to a different light curve shape term, ζ.

tent with the observed characteristics of known LBV systems, this does not mean that we have a viable physical model to explain these events. Rapid transient episodes in LBVs such as SN 2002kg and SN 2009ip may best be explained by a sudden ejection of an optically thick shell (e.g., Smith *et al.* 2010, 2011), or by some form of S Dor-type variability (Weis and Bomans 2005; Van Dyk *et al.* 2006; Foley *et al.* 2011), which may be driven by stellar pulsation rather than mass ejection (van Genderen *et al.* 1997; van Genderen 2001).

For massive stars such as η Carat its great eruption and the rapidly varying SN 2009ip, the effective photospheric radius during eruption must have been comparable to the orbit of Saturn (10^{14} cm; Davidson and Humphreys 1997; Smith *et al.* 2011; Foley *et al.* 2011). With observed photospheric velocities of order 500 km s^{-1} for such events, the dynamical timescale of the extended photosphere is on the order of tens to hundreds of days. Thus, if the very rapid light curves of both HFF14Spo events are indeed LBV eruptions, then they will be near the extreme limits of physical models for massive stellar eruptions.

2.2. *Recurrent Nova*

Novae are represented in Figure **??** as a grey band, which traces the maximum magnitude - rate of decline (MMRD) relation. Nova explosions occur in binary star systems in which the more massive star is a white dwarf that accretes matter from its companion, which may be a main sequence dwarf or evolved giant star overfilling its Roche Lobe. The white dwarf builds up a dense layer of H-rich material on its surface until the high pressure and temperature triggers nuclear fusion, resulting in a surface explosion that causes the white dwarf to brighten by several orders of magnitude, but does not completely disrupt the star. In a recurrent nova (RN) system, the mass transfer from the companion to the white dwarf restarts after the explosion, so the cycle may begin again and repeat after a period of months or years.

The seminal work of Zwicky (1936) and McLaughlin (1939) first showed that more luminous novae within the Milky Way tend to have more rapidly declining light curves, which is now the basis of the maximum-magnitude versus rate-of-decline (MMRD) relationship. The basic form of the MMRD relation has been theoretically attributed to a dependence of the peak luminosity on the mass of the accreting white dwarf (e.g. Livio 1992). Studies of extragalactic novae reaching as far as the Virgo cluster have shown that the MMRD relation is broadly applicable to all nova populations, though with significant scatter (e.g. Ciardullo *et al.* 1990; Della Valle and Livio 1995; Ferrarese *et al.* 2003; Shafter *et al.* 2011). Amidst that scatter, there may also be sub-populations of novae that deviate from the traditional MMRD form (Kasliwal *et al.* 2011b), and recurrent novae (RNe) in particular may be poorly represented by the MMRD (Shafter *et al.* 2011; Hachisu and Kato 2015)

In Figure **??**, the dark grey region follows the empirical constraints on the MMRD from Della Valle and Livio (1995), and the wider light grey band allows for the increased scatter about that relation that has been noted from more extensive surveys of novae in the Milky Way (Downes and Duerbeck 2000), M31 (Shafter *et al.* 2011) and elsewhere in the local group (Kasliwal *et al.* 2011b). Nova outbursts can exhibit decline times from $\sim$1 day to many months, so the timescale of the HFF14Spo light curves can easily be accommodated by the nova scenario. However, the peak luminosities inferred for the HFF14Spo events are larger than any known novae, perhaps by as much as 2 orders of magnitude.

Figure 3 shows a narrower slice of the same phase space as in Figure **??**, zooming in on the "fast and faint" region from the lower left corner. The observed constraints from the two published kilonova candidates are shown, which provide only lower limits on the peak luminosity (Tanvir *et al.* 2013), or the decline timescale (Perley *et al.* 2009). Two .Ia candidates are also plotted, SN 2002bj (Poznanski *et al.* 2010) and SN 2010X (Kasliwal *et al.* 2010). The sample of observed nova outbursts (shown as solid points) demonstrates the observed scatter about the MMRD relation.

One primary line of evidence supporting the nova hypothesis comes from the HFF14Spo light curves. Many RN light curves are similar in shape to the HFF14Spo episodes, exhibiting a sharp rise ($<$ 10 days in the rest-frame) and a similarly rapid decline. Figure 10 compares the HFF14Spo light curves to template light curves from RNe within our galaxy and in M31. There are 10 known RNe in the Milky Way galaxy, and 7 of these exhibit outbursts that decline rapidly, fading by 2 magnitudes in less than 10 days (Schaefer 2010) The gray shaded region in Figure 10 encompasses the V band light curve templates for all 7 of these events, from Schaefer (2010). The Andromeda galaxy (M31) also hosts at least one RN with a rapidly declining light curve. The 2014 eruption of this well-studied nova, M31N 2008a-12, is shown as a solid black line in Figure 10, fading by 2 mags in less than 3 days. This comparison demonstrates that the sudden disappearance of both of the HFF14Spo transient events is fully consistent with the eruptions of known RNe in the local universe.

The rise time of the HFF14Spo events is somewhat out of the ordinary for nova outbursts. In particular, for recurrent nova eruptions that decline rapidly ($t_2 < 10$ days) they tend to also reach peak brightness very quickly, on timescales $<$ 1 day (Schaefer 2010). The 2014 eruption of the rapid-recurrence nova M31N 2008a-12 reached maximum brightness in a little under 1 day (Darnley *et al.* 2015). However, the rise time for nova eruptions is poorly constrained, as rapid-cadence imaging is rarely secured until after an initial detection near peak brightness. Unlike the situation with a kilonova light curve, there is no a priori physical expectation for an especially rapid rise to peak in nova light curves.

Among the most luminous classical novae known, a similarly rapid decline time is not unheard of. For example, the bright nova M31N-2007-11d had $t_2 = 9.5$ days (Shafter *et al.* 2009). The extremely luminous nova SN 2010U had $t_2 = 3.5 \pm 0.3$ (Czekala *et al.* 2013). The nova L91 required at least 4 days to rise to maximum (Shafter *et al.* 2009), and then declined with $t_2 = 6 \pm 1$ days (della Valle 1991; Williams *et al.* 1994; Schwarz *et al.* 2001).

Another reason to consider the RN model is that it provides a natural explanation for having two separate explosions that are coincident in space but not in time. If HFF14Spo is a RN, then the two observed episodes can be attributed to two distinct nova eruptions, and the gravitational lensing time delay does not need to match the observed 8 month separation between the January

and August 2014 appearances.

Although *qualitatively* consistent with the 8-month separation, the RN model is strained by a quantitative assessment of the recurrence period. If HFF14Spo is indeed a RN at $z = 1$, then the recurrence timescale in the rest-frame is 120 ± 30 days ($3 - 5$ months), where the uncertainty accounts for the 1σ range of modeled gravitational lensing time delays. This would be a singularly rapid recurrence period, significantly faster than all 11 RNe in our own galaxy, which have recurrence timescales ranging from 15 years (RS Oph) to 80 years (T CrB). For the 5 galactic RNe with a rapidly declining outburst light curve (U Sco, V2487 Oph, V394 CrA, T CrB, and V745 Sco), the median recurrence timescale is 21 years. The fastest measured recurrence timescale belongs to the Andromeda galaxy nova M31N 2008a-12, which has exhibited a new outburst every year from 2009-2015 (Tang *et al.* 2014; Darnley *et al.* 2014, 2015; Henze *et al.* 2015a,b). Although this M31 record-holder demonstrates that very rapid recurrence is possible, classifying HFF14Spo as a RN would still require a very extreme mass transfer rate to accommodate the < 1 year recurrence.

Another major concern with the RN hypothesis for HFF14Spo is apparent in Figure 3, which shows that the two HFF14Spo events are substantially brighter than all known novae – perhaps by as much as 2 orders of magnitude. One might attempt to reconcile the HFF14Spo luminosity more comfortably with the nova class by assuming a significant lensing magnification for one of the two events. This would drive down the intrinsic luminosity, perhaps to $\sim 10^{40}$ erg s-1, on the edge of the nova region. However, this assumption implicitly moves the lensing critical curve to be closer to the HFF14Spo event in question. That pulls the critical curve away from the other HFF14Spo position, which makes that second event *more inconsistent* with observed nova peak luminosities.

2.2.1. *Physical Implications of the RN Model*

The physical limits of the RN model are best evaluated by combining the two key observables of recurrence period and peak brightness. In this examination we rely on a pair of papers that evaluated an extensive grid of nova models through multiple cycles of outburst and quiescence (Prialnik and Kovetz 1995; Yaron *et al.* 2005). Figure 12 plots first the RN outburst amplitude (the apparent magnitude between outbursts minus the apparent magnitude at peak) and then the peak luminosity against the log of the recurrence period in years. For the HFF14Spo events we can only measure a lower limit on the outburst amplitude, since the presumed progenitor star is unresolved, so no measurement is available at quiescence. Figure 12 shows that a recurrence period as fast as one year is expected only for a RN system in which the primary WD is both very close to the Chandrasekhar mass limit (1.4 $M_\odot$) and also has an extraordinarily rapid mass transfer rate ($\sim 10^{-6}$ $M_\odot$ yr^{-1}). The models of Yaron *et al.* (2005) suggest that such systems should have a very low peak amplitude (barely consistent with the lower limit for HFF14Spo) and a low peak luminosity (∼100 times less luminous than the HFF14Spo events).

The closest analog for the HFF14Spo events from the population of known RN systems is the nova M31N 2008a-12. Kato *et al.* (2015) provided a theoretical model that can account for the key observational characteristics of this remarkable nova: the very rapid recurrence timescale (<1 yr), fast optical light curve ($t_2 \sim 2$ days), and short supersoft x-ray phase (6-18 days after optical outburst Henze *et al.* 2015b). To match these observations, Kato *et al.* invoke a 1.38 $M_\odot$ white dwarf primary, drawing mass from a companion at a rate of 1.6×10^{-7} $M_\odot$ yr^{-1}. This is largely consistent with the theoretical expectations derived by Yaron *et al.* (2005), and reinforces the conclusion that a combination of a high mass white dwarf and efficient mass transfer are the key ingredients for rapid recurrence and short light curves. The one feature that can not be effectively explained with this scenario is the peculiarly high luminosity of the HFF14Spo events – even after accounting for the very large uncertainties. If the HFF14Spo transients are caused by a single RN system, then that progenitor system would be the most extreme WD binary yet known.

3. NON-EXPLOSIVE ASTROPHYSICAL TRANSIENTS

There are several categories of astrophysical transients that are not related to stellar explosions, and we find that these models cannot accommodate the observations of the HFF14Spo transients. We may first dismiss any of the category of *periodic* sources (e.g. Cepheids, RR Lyrae, or Mira variables) that exhibit regular changes in flux due to pulsations of the stellar photosphere. These variable stars do not exhibit sharp, isolated transient episodes that could match the HFF14Spo light curve shapes.

We can also rule out active galactic nuclei (AGN), in which brief transient episodes (a few days in duration) may be observed from X-ray to infrared wavelengths (e.g. Gaskell and Klimek 2003). The AGN hypothesis for HFF14Spo is disfavored for three primary reasons: First, AGN that exhibit short-duration transient events also typically exhibit slower variation on much longer timescales, which is not observed at either of the HFF14Spo locations. Second, the spectrum of the HFF14Spo host galaxy shows none of the broad emission lines that are often (though not always) observed in AGN. Third, an AGN would necessarily be located at the center of the host galaxy. In Section 8 we saw that there are minor differences in the host galaxy properties (i.e. rest-frame U-V color and mean stellar age) from the HFF14Spo-1 and HFF14Spo-2 locations to the center of the host galaxy at image 11.3 Although by no means definitive, this suggests that the HFF14Spo events were not located at the physical center of the host galaxy, and therefore are not related to an AGN. **TODO:** Update with MUSE results

Stellar flares provide a third very common source for optical transient events. Relatively mild stellar flares may be caused by magnetic activity in the stellar atmosphere, and the brightest flare events (so-called "superflares") may be generated by perturbations to the stellar atmosphere via interactions from a disk, a binary companion, or a planet. In these circumstances the stars release a *total* energy in the range of 10^{33} to 10^{38} erg over a span of minutes to hours (Balona 2012; Karoff *et al.*

2016). This falls far short of the observed energy release from the HFF14Spo transients, so we can also dismiss stellar flares as implausible for this source.

3.1. *Microlensing*

In the presence of strong gravitational lensing it is possible to generate a transient event from lensing effects alone. In this case the background source has a steady luminosity but the relative motion of the source, lens, and observer causes the magnification of that source to change rapidly with time.

A commonly observed example is the microlensing of a bright background source (a quasar) by a galaxy-scale lens (Wambsganss 2001; Kochanek 2004). In this optically thick microlensing regime, the lensing potential along the line of sight to the quasar is composed of many stellar-mass objects. Each compact object along the line of sight generates a separate critical lensing curve, resulting in a complex web of overlapping critical curves. As all of these lensing stars are in motion relative to the background source, the web of caustics will shift across the source position, leading to a stochastic variability on timescales of months to years. This scenario is inconsistent with the observed data, as the two HFF14Spo events were far too short in duration and did not exhibit the repeated "flickering" variation that would be expected from optically thick microlensing.

A second possibility is through an isolated strong lensing event with a rapid timescale, such as a background star crossing over a lensing critical curve. This corresponds to the optically thin microlensing regime, and is similar to the "local" microlensing light curves observed when stars within our galaxy or neighboring dwarf galaxies pass behind a massive compact halo object (Paczynski 1986; Alcock *et al.* 1993; Aubourg *et al.* 1993; Udalski *et al.* 1993). In the case of a star crossing the caustic of a smooth lensing potential, the amplification of the source flux would increase (decrease) with a characteristic $t^{-1/2}$ profile as it moves toward (away from) the caustic. This slowly evolving light curve transitions to a very sharp decline (rise) when the star has moved to the other side of the caustic (Schneider and Weiss 1986; MiraldaEscude 1991). With a more complex lens comprising many compact objects, the light curve would exhibit a superposition of many such sharp peaks (Lewis *et al.* 1993).

To generate an isolated microlensing event, the background source would have to be the dominant source of luminosity in its environment, meaning it must be a very bright O or B star with mass of order 10 $M_\odot$. Depending on its age, the size of such a star would range from a few to a few dozen times the size of the sun. The net relative transverse velocity would be on the order of a few 100 km/s, which is comparable to the orbital velocity of stars within a galaxy or galaxies within a cluster. In the case of a smooth cluster potential—the characteristic timescale of such an event would be on the order of hours or days Chang and Refsdal (1979, 1984); MiraldaEscude (1991), which is in the vicinity of the timescales observed for the HFF14Spo events. However, if we apply this scenario to the MACS J0416.1-2403 field, we can not plausibly generate two events with similar decay timescales at distinct locations on the sky. This is because a caustic-crossing transient event must necessarily appear at the location of the lensing critical curve, but in this case the critical curve most likely passes between the two observed HFF14Spo locations. At best, a caustic crossing could account for only one of the HFF14Spo events, not both.

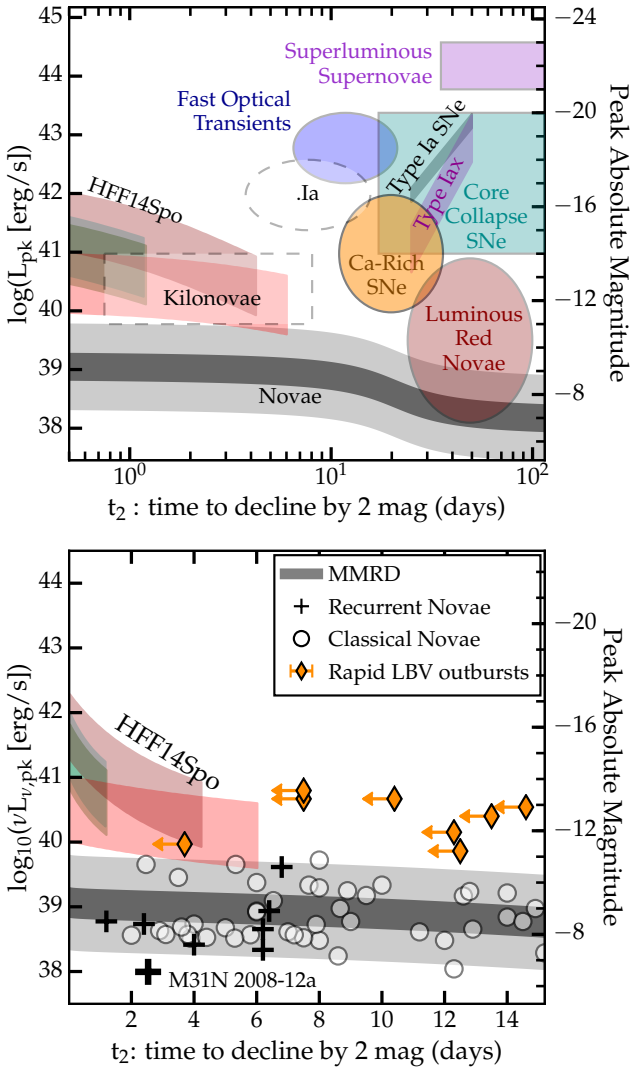

FIG. 3.— Peak luminosity vs. decline time for HFF14Spo and other rapidly declining recurrent transients. Constraints for HFF14Spo-1 and HFF14Spo-2 are plotted as overlapping colored bands, as in Figure **??**. Grey bands show the MMRD relation for classical novae, as in Figure **??**. Circles mark the observed peak luminosities and decline times for classical novae from the Milky Way (Downes and Duerbeck 2000), M31 (Shafter *et al.* 2011), and the local group (Kasliwal *et al.* 2011a). Black '+' symbols mark the 7 rapidly declining Recurrent Novae from our own galaxy (Schaefer 2010), and the large cross labeled at the bottom shows the rapid recurrence nova M31N 2008-12a (Tang *et al.* 2014; Darnley *et al.* 2015). Each orange diamond marks a separate short transient event from the two rapid LBV outburst systems, SN 2009ip (Pastorello *et al.* 2013) and NGC3432-LBV1 (a.k.a. SN 2000ch Pastorello *et al.* 2010). These LBV events provide only upper limits on the decline time due to limited photometric sampling.

4. DISCUSSION

We have found that three models offer plausible explanations for the HFF14Spo events: these transients are due to a RN

Our preferred explanation for the HFF14Spo events

is that we have observed two distinct eruptive episodes from a massive LBV star. The light curve shape is consistent with rapid LBV eruptions seen in systems such as SN 2009ip and NGC 3432-LBV1. The peak luminosity and recurrence timescale are also within the bounds of what has been observed from nearby LBVs. The HFF14Spo episodes may have been among the fastest and most luminous of any rapid LBV events yet observed. However, no other rapid LBV outbursts have yet been observed with such a high cadence, so the detailed light curve shape can not be rigorously compared against other events. In this scenario, the HFF14Spo LBV system would most likely have exhibited multiple eruptions over the last few years, but most of them were missed, as they landed within the large gaps of the *HST* Frontier Fields imaging program.

We speculate that the very luminous and very fast HFF14Spo transients may be driven by extreme mass eruption events or an extreme form of stellar pulsation. Both of these mechanisms are likely to occur in LBV progenitor stars, but we do not have a robust model for precisely how LBV eruptions are generated. This is a topic in need of significant theoretical work, with the end goal being a comprehensive physical model that accommodates both the η Car-like great eruptions and the S Dor-type variation of LBVs. The HFF14Spo events are extreme in several dimensions, and will only add to this theoretical challenge.

The authors thank (ML,LC,DH...) for helpful discussion of this paper.

Financial support for this work was provided to S.A.R. by NASA through grant HST-GO-13386 from the Space Telescope Science Instittute (STScI), which is operated by Associated Universities for Research in Astronomy, Inc. (AURA), under NASA contract NAS 5-26555.

5. METHODS

6. OBSERVATIONS

The transient HFF14Spo was discovered in HST imaging collected as part of the Hubble Frontier Fields (HFF) survey (HST-PID:13496, PI:Lotz), a multi-cycle program observing 6 massive galaxy clusters and associated "blank sky" parallel fields. Several HST observing programs have provided additional observations supplementing the core HFF program. One of these is the FrontierSN program (HST-PID:13386, PI:Rodney), which aims to identify and study explosive transients found in the HFF and related programs. The FrontierSN team discovered HFF14Spo in two separate HFF observing campaigns on the galaxy cluster MACS J0416.1-2403 (hereafter, MACS0416). The first was an imaging campaign in January, 2014 during which the MACS0416 cluster field was observed in optical bands using the Advanced Camera for Surveys Wide Field Camera (ACS-WFC). The second concluded in August, 2014, and imaged the cluster with the infrared detector of HST's Wide Field Camera 3 (WFC3-IR).

To discover transient sources, the FrontierSN team processes each new epoch of HST data through a difference imaging pipeline[3], using archival HST images to provide reference images (templates) which are subtracted from the astrometrically registered HFF images. In the case of MACS0416, the templates were constructed from images collected as part of the Cluster Lensing And Supernova survey with Hubble (CLASH, HST-PID:12459, PI:Postman). The resulting difference images are visually inspected for new point sources, and any new transients of interest (primarily supernovae, SNe) are followed up with additional HST imaging or ground-based spectroscopic observations as needed. For a more complete description of the operations of the FrontierSN program, see Rodney *et al.* (2015).

The follow-up observations for HFF14Spo included HST observations in infrared and optical bands using the WFC3-IR and ACS-WFC detectors, respectively, as well as spectroscopy of the HFF14Spo host galaxy using three instruments on the Very Large Telescope (VLT). Observations with the VLT's X-shooter cross-dispersed echelle spectrograph (Vernet *et al.* 2011) were taken on October 19th, 21st and 23rd, 2014 (Program 093.A-0667(A), PI: J. Hjorth) with the slit centered on the position of HFF14Spo 2. The total integration time was 4.0 hours for the NIR arm of X-shooter, 3.6 hours for the VIS arm, and 3.9 hours for the UVB arm. The spectrum did not provide any detection of the transient source itself (as we will see below, it had already faded back to its quiescent state by that time). However, it did provide an unambiguous redshift for the host galaxy of $z = 1.0054 \pm 0.0002$ from Hα and the O[II] doublet in data from the NIR and VIS arms, respectively. These line identifications are consistent with two measures of the photometric redshift of the host: $z = 1.00 + -0.02$ from the BPZ algorithm (Benítez 2000), and $z = 0.92 \pm 0.05$, derived using the EAZY program (Brammer *et al.* 2008).

Additional VLT observations were collected using the Visible Multi-object Spectrograph (VIMOS Le Fèvre *et al.* 2003), as part of the CLASH-VLT large program

[3] `https://github.com/srodney/sndrizpipe`

(Program 186.A-0.798; P.I.: P. Rosati; Rosati *et al.* 2014)), which collected ∼4000 reliable redshifts over 600 arcmin^2 in the MACS J0416.1-2403 field (Grillo *et al.* 2015; Balestra *et al.* 2015). These massively multi-object observations could potentially have provided confirmation of the redshift of the HFF14Spo host galaxy with separate spectral line identifications in each of the three host galaxy images. On the MACS J0416.1-2403 field this program collected 1 hr of useful exposure time in good seeing conditions with the Low Resolution Blue grism. Unfortunately, the wavelength range of this grism (3600-6700 å) does not include any strong emission lines for a source at z=1.0054, and the signal-to-noise (S/N) was not sufficient to provide any clear line identifications for the three images of the HFF14Spo host galaxy.

The VLT Multi Unit Spectroscopic Explorer (MUSE; Henault *et al.* 2003; Bacon *et al.* 2012) observed the MACS J0416.1-2403 field as part of the SPECIFY PROGRAM INFO AND ADD CITATIONS HERE on DATES OF OBSERVATION AND EXPOSURE TIMES. These observations also confirmed the redshift of the host galaxy with clear detection of the O[II] doublet. Importantly, since MUSE is an integral field spectrograph, these observations also provided a confirmation of the redshift of the third image of the host galaxy, 11.3, with a matching O[II] line at the same wavelength.

The MUSE data also provide spatial resolution of the O[II] signal, allowing examination of possible substructure in the host images 11.1 and 11.2 (see Section 8. As reported in Table **??** O[II] lines do not exhibit any discernible gradient across the host galaxy images in terms of the wavelength of line centers, full width at half maximum, or the intensity ratio of the two components of the doublet. Thus, the O[II] measurements from MUSE can not be used to distinguish either HFF14Spo location from the other, or to definitively answer whether either position is coincident with the center of the host galaxy. We conclude that it is plausible but not certain that the two HFF14Spo events arose from the same physical location in the host galaxy.

A final source of spectroscopic information relevant to HFF14Spo is the Grism Lens Amplified Survey from Space (GLASS; PID: HST-GO-13459; PI:T. Treu Schmidt *et al.* 2014; Treu *et al.* 2015). The GLASS program collected slitless spectroscopy on the MACS J0416.1-2403 field using the WFC3-IR G102 and G141 grisms on *HST*. As with the VLT VIMOS data, the three sources identified as images of the HFF14Spo host galaxy are too faint in the GLASS data to provide any useful line identifications. There are also no other sources in the GLASS redshift catalog[4] that have a spectroscopic redshift consistent with z=1.0054.

Table **TODO:** (add a table with photometry) and Figure 2 present photometry of the HFF14Spo events from all available HST observations. The flux was measured on difference images, first using aperture photometry with a 0.″3 radius, and also by fitting with an empirical point spread function (PSF). The PSF model was defined using HST observations of the G2V standard star P330E, observed in a separate calibration program. A separate PSF model was defined for each filter, but owing to the long-term stability of the HST PSF we used the same model in all epochs. All of the aperture and PSF fitting photometry was carried out using the `PythonPhot` software package (Jones *et al.* 2015).

[4] `http://glass.astro.ucla.edu/`

7. LIGHT CURVES

Due to the rapid decline timescale, no observations were collected for either event that unambiguously show the declining portion of the light curve. Therefore, we must make some assumption for the shape of the light curve in order to quantify the peak luminosity and the corresponding timescales for the rise and the decline. We first approach this with a simplistic model that is piecewise linear in magnitude vs time. Figure 4 shows examples of the resulting fits for the two events. For each fit we use only the data collected within 3 days of the brightest observed magnitude, which allows us to fit a linear rise separately for the F606W and F814W light curves for HFF14Spo-1 and the F125W and F160W light curves for HFF14Spo-2. To quantify the covariance between the true peak brightness, the rise time and the decline timescale, we use the following procedure:

1. make an assumption for the date of peak, $t_{\rm pk}$;
2. measure the peak magnitude at $t_{\rm pk}$ from the linear fit to the rising light curve data;
3. assume the source reaches a minimum brightness (maximum magnitude) of 30 AB mag at the epoch of first observation after the peak;
4. draw a line for the declining light curve between the assumed peak and the assumed minimum brightness;
5. use that declining light curve line to measure the timescale for the event to drop by 3 magnitudes, t_3;
6. make a new assumption for $t_{\rm pk}$ and repeat.

As shown in Figure 4, the resulting piece-wise linear fits are simplistic, but nevertheless approximately capture the observed behavior for both events. Furthermore, since this toy model is not physically motivated, it allows us to remain agnostic for the time being as to the astrophysical source(s) driving these transients. From these fits we can see that HFF14Spo-1 most likely reached a peak magnitude between 25 and 26.5 AB mag in both F814W and F435W, and had a decline timescale t_3 of less than 2 days in the rest-frame. The observations of HFF14Spo-2 provide less stringent constraints, but we see that it had a peak magnitude between 23 and 26.5 AB mag in F160W and exhibited a decline time of less than seven days. These fits also illustrate the generic fact that a higher peak brightness corresponds to a longer rise time and a faster decline timescale, independent of the specific model used. Changes to the arbitrary constraints we placed on these linear fits do not substantially affect the results. For example, the relationship between peak brightness and decline time is not strongly affected by adjusting the assumed maximum post-peak magnitude or changing the number of pre-peak data points used for the rising light curve fits.

TABLE 2
Measurements of the O[II] λλ3626,3629 lines from HFF14Spo host galaxy images 11.1 and 11.2[a]

Aperture ID	R.A. J2000 (degrees)	Dec. J2000 (degrees)	distance to HFF14Spo-2 (Arcsec)	O[II] λ3726 Flux ($\mathrm{erg\,s^{-1}\,cm^{-2}}$)	$\lambda_{\mathrm{center}}$ (Å)	FWHM (Å)	O[II] λ3729 Flux ($\mathrm{erg\,s^{-1}\,cm^{-2}}$)	$\lambda_{\mathrm{center}}$ (Å)	FWHM (Å)	Line Ratio
1	64.039371	-24.070450	-1.54	2.19e-18	7472.37	4.00	3.57e-18	7478.17	4.00	1.63
2	64.039218	-24.070345	-0.88	4.73e-18	7472.16	4.00	5.30e-18	7478.12	3.40	1.12
3	64.039078	-24.070264	-0.30	5.05e-18	7472.29	4.00	6.10e-18	7478.27	3.73	1.21
4	64.038921	-24.070163	0.39	4.22e-18	7472.19	4.00	5.74e-18	7478.08	3.59	1.36
5	64.038785	-24.070078	0.97	3.86e-18	7472.25	4.00	6.56e-18	7478.19	4.00	1.70
6	64.038637	-24.069958	1.65	4.80e-18	7472.51	4.00	5.42e-18	7478.07	2.69	1.13
7	64.038501	-24.069865	2.24	4.60e-18	7472.57	3.43	5.74e-18	7478.17	3.20	1.25
8	64.038352	-24.069752	2.92	4.70e-18	7472.54	3.54	6.22e-18	7478.16	2.95	1.32
9	64.038229	-24.069648	3.50	3.26e-18	7472.83	2.80	5.79e-18	7478.16	2.84	1.77
10	64.038076	-24.069532	4.19	2.44e-18	7473.01	2.57	3.22e-18	7478.10	2.73	1.32
Spo-1	64.038565	-24.069939	1.90	4.30e-18	7472.55	3.13	5.49e-18	7478.01	2.89	1.28
Spo-2	64.038998	-24.070241	0.00	4.37e-18	7472.46	4.00	6.10e-18	7478.22	3.79	1.40

[a]Properties of the of the O[II] lines were derived from 1-D spectra extracted from the MUSE data cube at 10 locations spaced 0.″6 apart along the length of the arc that comprises images 11.1 and 11.2 of the HFF14Spo host galaxy. Each extraction used an aperture of 0.″6 radius, centered on the mid-line of the host galaxy arc. The integrated line flux, observed wavelength of line center ($\lambda_{\mathrm{center}}$), and full width at half maximum (FWHM) were found by fitting a Gaussian profile to each component of the doublet.

7.1. *Color Curves*

At redshift $z = 1$ the observed optical and infrared bands translate to rest-frame ultraviolet (UV) and optical wavelengths, respectively. To derive rest-frame UV and optical colors from the observed photometry, we start with the measured magnitude in a relatively blue band (F435W and F606W for HFF14Spo-1 and F105W, F125W, F140W for HFF14Spo-2). We then subtract the coeval magnitude for a matched red band (F814W for HFF14Spo-1, F125W or F160W for HFF14Spo-2), derived from the linear fits to those bands. To adjust these to rest-frame filters, we apply K corrections (following Hogg *et al.* 2002), which we compute by defining a crude SED via linear interpolation between the observed broad bands for each transient event at each epoch. For consistency with past published results, we include in each K correction a transformation from AB to Vega-based magnitudes. The resulting UV and optical colors are plotted in Figure 5. Both HFF14Spo-1 and HFF14Spo-2 show little or no color variation over the period where color information is available.

8. HOST GALAXY

Before we can examine astrophysical models that might explain these transients, we first must examine whether the two transients originated from the same physical location in the source plane. One way to test this is to compare the properties of the HFF14Spo host galaxy at the location of each event. To that end, we used the technique of "pixel-by-pixel" SED fitting as described in Hemmati *et al.* (2014) to determine rest-frame colors and stellar properties in a single resolution element centered at each transient location. For this purpose we used the deepest possible stacks of HST images, comprising all available data except those images where the transient events were present. The resulting maps of stellar population properties are shown in Figure 6. Table 3 reports measurements of the three derived stellar population properties (color, mass, age) from host images 11.1, 11.2 and 11.3. In 11.1 and 11.2 these measurements were extracted from the central pixel at the location of each of the two HFF14Spo events. Assuming the lensing magnification here ranges from $\mu = 10$ to 100 (see Section 9, this corresponds to a size on the source plane between 6 and 600 pc^2. For host image 11.3 we report the stellar population properties dervide from the pixel at the center of the galaxy. With a magnification of ∼3 to 5, the extraction region covers roughly 2000 to 6000 pc^2.

TABLE 3
Properties of the local stellar population in the HFF14Spo host galaxy, from SED fitting.

Host image:	11.1	11.2	11.3
Location:	HFF14Spo-2	HFF14Spo-1	center
$(U-V)_{\mathrm{rest}}$	$0.69^{+0.2}_{-0.05}$	$0.52^{+0.15}_{-0.10}$	0.39±0.05
$\log[\Sigma(M_*/\mathrm{M}_\odot)]$	7.14 ± 0.15	7.14 ± 0.15	7.04 ± 0.10
Age (Gyr)	0.292±0.5	0.290±0.5	0.292±0.5

The reported uncertainties for these derived stellar properties in Table 3 reflect only the measurement errors from the SED fitting, and do not attempt to quantify potential systematic biases. Such biases could arise, for example, from color differences in the background light, which is dominated by the cluster galaxies and varies significantly across the MACS J0416.1-2403 field. Such a bias might shift the absolute values of the parameter scales for any given host image (e.g., making the galaxy as a whole appear bluer, more massive and younger). However, the gradients across any single host image are unlikely to be driven primarily by such systematics.

Figure 6 and Table 3 show that the measured values of the color, stellar mass, and age at the two HFF14Spo locations are mutually consistent. Thus, it is plausible to assume that the two positions map back to the same physical location at the source plane. Comparing those two locations to the center of the galaxy as defined in image 11.3, we see only a mild tension in the rest-frame U-V color. This comparison therefore can not quantitatively rule out the possibility that the two transient events are located at the center of the galaxy. However, the maps shown in Figure 6 do show a gradient in both U-V color and stellar age. For both images 11.1 and 11.2 the bluest

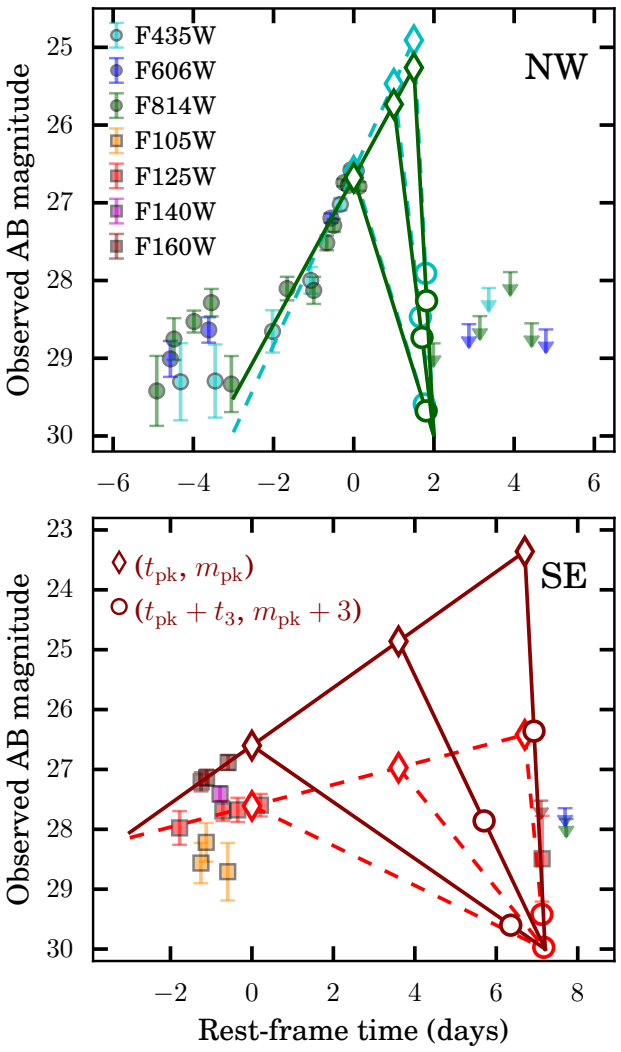

FIG. 4.— Piece-wise linear fits to the HFF14Spo light curves, used to measure the rise time and decay time of the two events. The HFF14Spo-1 light curve is shown in the top panel, and HFF14Spo-2 in the bottom. Filled points with error bars plot the observed brightness of each event in AB magnitudes as a function of rest-frame time (for $z = 1.0054$). Piece-wise linear fits are shown for the four bands that have enough points for fitting: in the top panel fits are plotted for the F814W band (solid green lines) and the F435W band (dashed cyan lines), while in the bottom panel fits are shown for F160W (solid maroon) and F125W (dashed scarlet). Open diamonds in each panel show three examples of assumptions for the time of peak brightness, t_{pk} (i.e. the position where the rising piece of the linear fit ends). Open circles mark the corresponding point, $t_{pk} + t_3$, at which the fading transient would have declined in brightness by 3 magnitudes. See text for details on the fitting procedure.

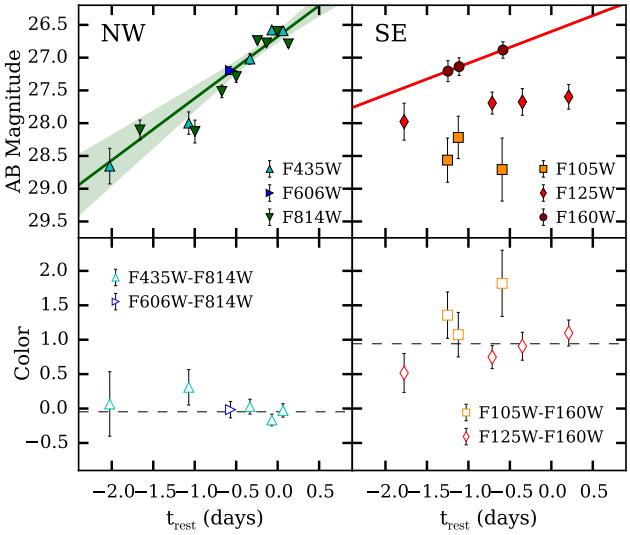

FIG. 5.— Observed colors for the HFF14Spo events. Filled points plotted in the top panels show observed AB magnitudes for the HFF14Spo-1 and HFF14Spo-2 events from -3 rest-frame days before the date of observed peak brightness. Solid lines and shaded regions show linear fits to the data in the F814W and F160W bands. Open points in the bottom panels show observed colors in the rest-frame bands. For each color the magnitude in the bluer band is the directly measured value, and the magnitude in the redder band is interpolated from the linear fits shown in the top panel. All colors are consistent with showing no evolution over the rising portion of each light curve.

and youngest stars (U-V∼0.3, τ ∼280 Myr) are localized in knots near the extreme ends of each image, well separated from either of the HFF14Spo transient events. In the less distorted host image 11.3 the bluer and younger stars are concentrated near the center. Taken together, these color and age gradients suggest that the two transients are not coincident with the center of their host galaxy.

In addition to the HST imaging data, we also have spatially resolved spectroscopy from the MUSE integral field data. The only significant spectral line feature for the HFF14Spo host is the O[II] ($\lambda\lambda$ 3727, 3729) doublet, observed at 7474 and 7478 Å. Figure 7 shows the observed O[II] lines at 10 positions along the length of the arc, which comprises images 11.1 and 11.2. At each position the lines were extracted using apertures with a radius of 0.6″, so adjacent extractions are not independent, but extractions at the center of 11.1 and the center of 11.2 have no overlap. Each extraction has been normalized to show a peak line flux at unity, so that the line profiles and the doublet line ratios may be more easily compared. **TODO:** Make a table of line ratios and say something about whether spock1 and spock2 are consistent with being coincident at the source plane

9. GRAVITATIONAL LENS MODELS

The five lens models used to provide estimates of the plausible range of magnifications and time delays are:
NOTE: THESE DESCRIPTIONS ARE PROBABLY INCORRECT. MODELERS, PLEASE FIX AS NEEDED.

- *Diego:* Created with the `WSLAP+` software (Sendra *et al.* 2014): Weak and Strong Lensing Analysis Package plus member galaxies (Note: no weak-lensing constraints used for this MACS J0416 model). Interactive online model exploration available at `http://www.ifca.unican.es/users/jdiego/LensExplorer`.
- *Jauzac:* The model of Jauzac *et al.* (2014), generated with the `LENSTOOL` software (Jullo *et al.*

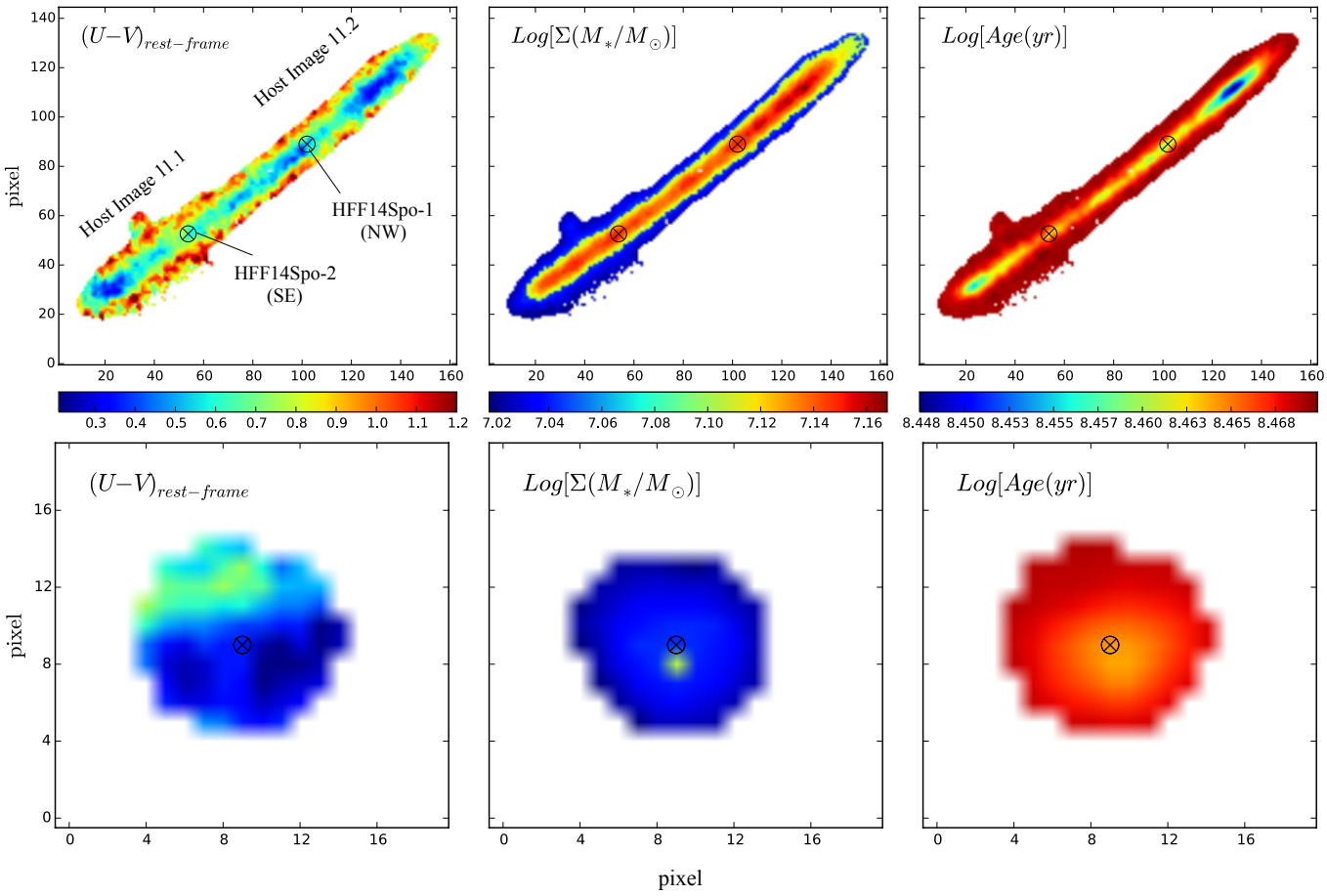

FIG. 6.— Stellar population properties of the HFF14Spo host galaxy, derived from "pixel-by-pixel" SED fitting. The top row shows maps for the adjacent host images 11.1 and 11.2, and the bottom panels show image 11.3. From left to right the panels present the rest-frame (U-V) color, the stellar surface mass density, Σ, and the mean age of the stellar population in Gyr. Markers in the top row denote the positions of the two HFF14Spo transient events. Markers in the bottom panels are at the center of host image 11.3.

2007),[5] using strong- and weak-lensing constraints. This model makes a light-traces-mass assumption and parameterizes cluster components using Navarro-Frenk-White (NFW) density profiles (Navarro *et al.* 1997).

- *Kawamata:* The model of Kawamata *et al.* (2015), built using the `GLAFIC` software[6] with strong-lensing constraints.
- *Williams:* An adaptive grid model developed using the `GRALE` software tool (Liesenborgs *et al.* 2006, 2007; Mohammed *et al.* 2014), which uses a genetic algorithm to reconstruct the cluster mass profile with an arrangement of projected Plummer 1911 density profiles.
- *Zitrin:* A model with strong- and weak-lensing constraints, built using the PIEMD+eNFW parameterization for density profiles as in Zitrin *et al.* (2009).

The *Williams* and *Zitrin* models were originally distributed as part of the Hubble Frontier Fields lens modeling project,[7] in which models were generated based on data available before the start of the HFF observations to enable rapid early investigations of lensed sources. The *Jauzac* model is an updated version of the model developed for that HFF modeling effort by the CATS team. In all cases the lens modelers made use of strong-lensing constraints (multiply-imaged systems and arcs) derived from HST imaging collected as part of the CLASH program (PI:Postman, HST PID:12459, Postman *et al.* 2012). These models also made use of spectroscopic redshifts in the cluster field from Mann and Ebeling (2012), Christensen *et al.* (2012), and Grillo *et al.* (2015). Input weak-lensing constraints also made use of data collected at the Subaru Telescope by PI K. Umetsu (in prep) and archival imaging. Priewe *et al.* (2016) provides a more complete description of the methodology of each model and a comparison of the magnification predictions and uncertainties across the entire MACS J0416.1-2403 field.

Figure 9 presents probability distributions derived from these models for the three magnifications and two

[5] `http://projects.lam.fr/repos/lenstool/wiki`
[6] `http://www.slac.stanford.edu/~oguri/glafic/`
[7] For more details, see `https://archive.stsci.edu/prepds/frontier/lensmodels/`

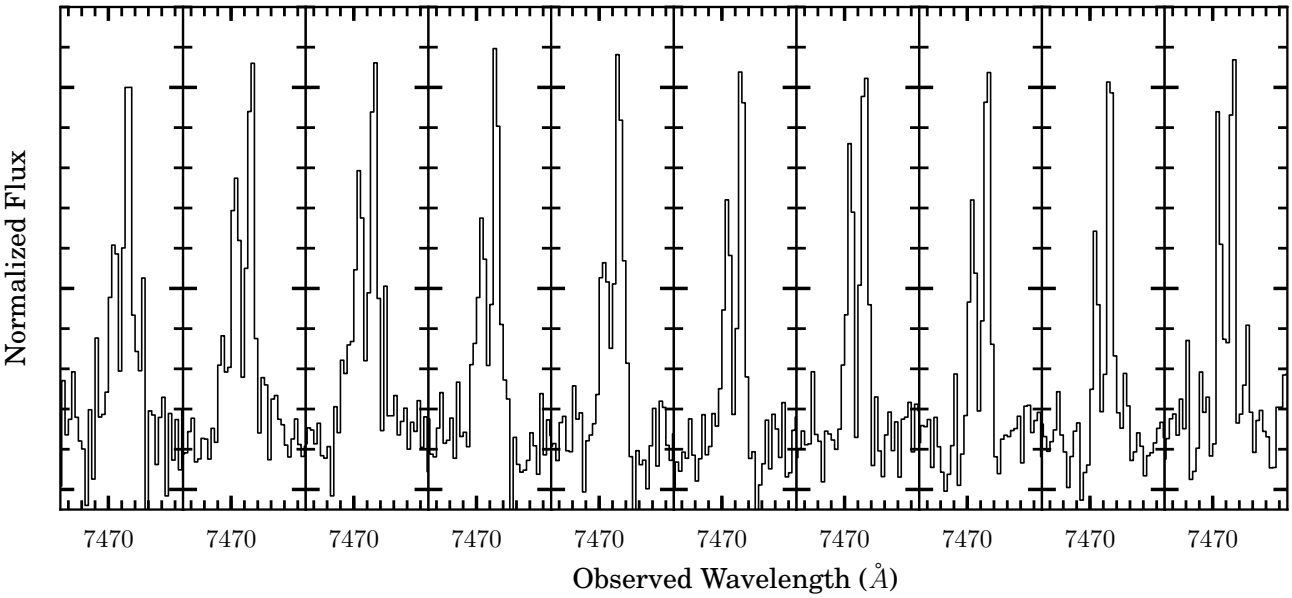

FIG. 7.— The [OII] line, observed with MUSE, at a series of ten locations along the HFF14Spo host galaxy arc. **TODO:** add in values for the [OII] doublet line ratio **TODO:** Add in panels showing [OII] lines from 11.3 and the spock locations. **TODO:** add in a panel showing the extraction apertures.

time delay values of interest. These distributions were derived by combining the Monte Carlo chains from the Jauzac, Oguri, Williams and Zitrin models, with weighting applied to account for the different number of model iterations in each chain. Four of the five models agree that host image 11.3 is the leading image, appearing some 2–6 years before the other two images. The models do not agree on the arrival sequence of images 11.1 and 11.2: some have the NW image 11.2 as a leading image, and others have it as a trailing image. However, the models do consistently predict that the separation in time between those two images should be roughly in the range of 1 to 60 days.

10. STELLAR EXPLOSION MODELS

Most optical transient events observed in extragalactic surveys can be explained as stellar explosions of one type or another. As the HFF14Spo transients do not easily fall within familiar categories, a useful starting point for comparing them to known stellar explosion categories is to examine the phase space of peak luminosity versus decline time (see, e.g., Kasliwal *et al.* 2010). To infer the luminosity and decline time for each HFF14Spo event, we combine the linear fits to the light curves (shown in Figure 4) with the predicted range of lensing magnifications (Figure 9. For any assumed value for the time of peak brightness, the light curve fits give us an estimate of the "observed" peak magnitude and a corresponding rise-time and decline-time measurement. We then convert this extrapolated peak magnitude to a luminosity (e.g., νL_ν in erg s^{-1}) by first correcting for the luminosity distance assuming a standard ΛCDM cosmology, and then accounting for an assumed lensing magnification, μ. At the end of all this, we have a grid of possible peak luminosities for each event as a function of magnification and time of peak (or, equivalently, the decline time).

Figures **??** and 3 show the resulting constraints on the peak luminosity and the decline time, which we quantify as t_2, the time over which the transient declines by 2 magnitudes. Shaded green and red bands represent the HFF14Spo-1 and HFF14Spo-2 events, respectively, and in each case they incorporate the allowed range for time of peak (see Figure 4) and the lensing magnification ($10 < \mu < 100$) as reported in Table 1. The two events are largely consistent with each other, and if both events are representative of a single system (or a homogeneous class) then the most likely peak luminosity and decline time (the region with the most overlap) would be $L_{\rm pk} \sim 10^{41}$ ergs/s and $t_3 \sim 1.8$ days.

10.1. *Supernova-like Transients*

The colored regions along the right side of Figure **??** mark the luminosity and decline times for SNe and SN-like transients. This includes the familiar luminosity-decline relation of Type Ia SNe (Phillips 1993) and the broad heterogeneous class of Core Collapse SNe, as well as less well-understood classes such as Superluminous SNe (Gal-Yam 2012; Arcavi *et al.* 2016), Type Iax SNe (Foley *et al.* 2013), fast optical transients (Drout *et al.* 2014), Ca-rich SNe (Filippenko *et al.* 2003; Perets *et al.* 2011; Kasliwal *et al.* 2012), and Luminous Red Novae (also called intermediate luminosity red transients; Munari *et al.* 2002; Kulkarni *et al.* 2007; Kasliwal *et al.* 2011a). The HFF14Spo events are incompatible with all of these explosion categories, owing to the very rapid rise and fall of both HFF14Spo light curves, and their relatively low peak luminosities of $\sim 10^{41}$ erg s^{-1}.

Dashed boxes in Figure **??** represent categories of "SN-like" stellar explosions that have been theoretically predicted and extensively modeled, but for which very few viable candidates have actually been observed. Both of these categories come closer to matching the observed characteristics of the two HFF14Spo events, so they warrant closer scrutiny.

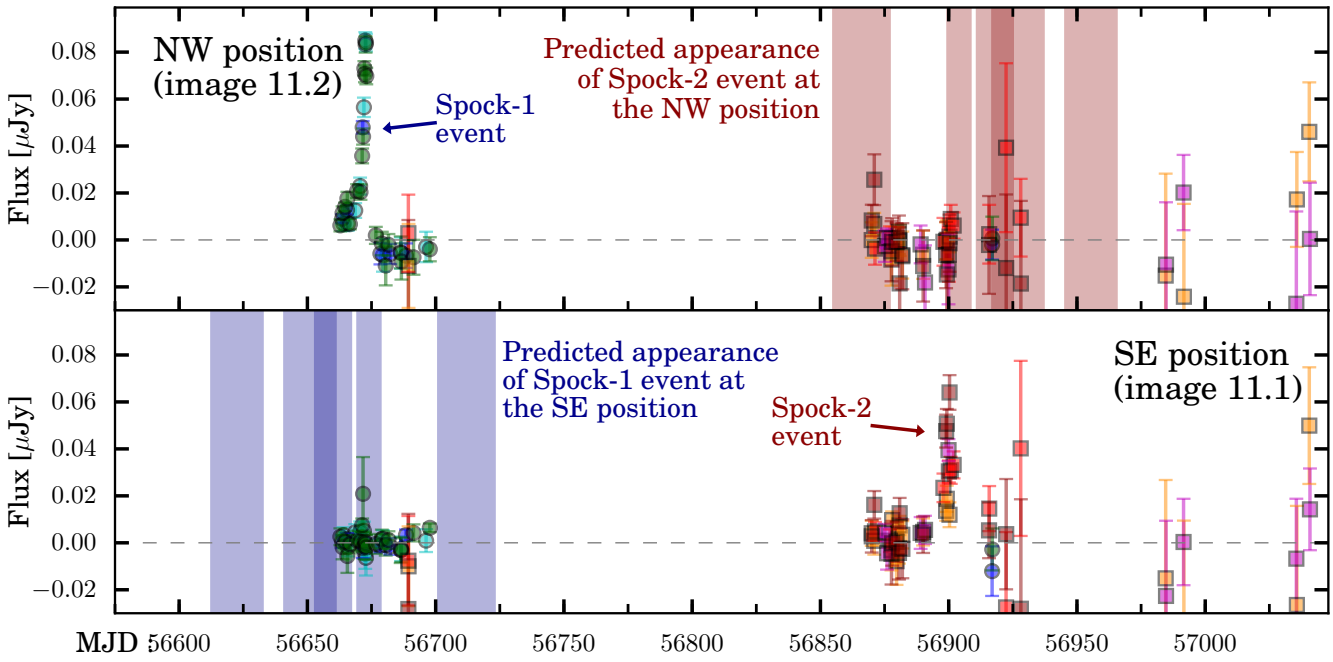

FIG. 8.— Predictions for the reappearance episodes of both HFF14Spo-1 and HFF14Spo-2 due to gravitational lensing time delays, as listed in Table 1. The top panel shows photometry collected at the NW position (host galaxy image 11.2) where the first event (HFF14Spo-1, labeled spock1) appeared in January, 2014. Optical measurements from ACS are in blue and green, and infrared observations from WFC3-IR are in red and orange, as in Figure 2. Each blue bar in the lower panel shows one lens model prediction for the dates when that same physical event (HFF14Spo-1) would have also appeared in the SE location (galaxy image 11.1), due to gravitational lensing time delay. The lower panel plots photometry from the SE position (11.1). On the right side we see the second observed event (HFF14Spo-2, labeled spock2). The red bars above show model predictions for when the NW host image 11.2 would have exhibited the gravitationally delayed image of the HFF14Spo-2 event. The width of each bar encompasses the 68% confidence region for a single model, and darker regions indicate an overlap from multiple models.

10.1.1. *Kilonova*

Also called a "macronova" or "mini-supernova," this is a theorized optical transient that may be generated by the merger of a neutron star (NS) binary. Such a NS+NS merger can drive a relativistic jet that may be observed as a Gamma Ray Burst (GRB) and would emit gravitational waves. These may also be accompanied by a very rapid optical light curve (the kilonova component) that is driven by the radioactive decay of r-process elements in the ejecta (Li and Paczyński 1998; Kulkarni 2005). To date there are two cases of fast optical transients associated with GRB events, which have been interpreted as possible kilonovae (Perley *et al.* 2009; Tanvir *et al.* 2013). The HFF14Spo transients fall within the range of theoretically predicted peak luminosity and decline times for kilonovae. However, the rise time for the HFF14Spo-1 event is at least 5 days in the rest-frame, which is significantly longer than the < 1 day rise expected for a kilonova (e.g. Metzger *et al.* 2010; Barnes and Kasen 2013; Kasen *et al.* 2015). Furthermore, both HFF14Spo events are either significantly fainter or faster than the optical light curves for the two existing kilonova candidates.

10.1.2. *.Ia Supernova*

The dashed oval in Figure **??** represents the ".Ia" class of He shell explosions (Bildsten *et al.* 2007). These are theorized to arise from AM Canum Venaticorum (AM CVn) systems, which are binary star systems transferring He onto a C/O or O/Ne WD primary (Warner 1995; Nelemans and Tout 2005). Bildsten *et al.* (2007) argued that these systems can build up enough He on the surface of the WD to trigger a thermonuclear runaway and possibly a detonation. A typical AM CVn system could produce ∼10 He shell flashes over $\sim 10^6$ yr, while the He mass transfer rate is slow enough to admit thermally unstable burning in the WD's accreted He shell. The final He shell flash is the brightest, and is what we refer to as the .Ia event. This last explosion may or may not lead to a detonation of the WD core (the double detonation scenario; Nomoto 1982a,b; Woosley and Weaver 1986, 1994).

Theoretical .Ia models suggest that the light curves would be quite bright, reaching a peak luminosity of $\sim 10^{42}$ erg s^{-1}. That is comparable to the brightness of a normal SN, but the .Ia light curves would decline much more quickly. After an initial short peak (3-5 days) driven by the rapid radioactive decay of ^{48}Cr and ^{52}Fe at the exterior of the ejecta, a secondary decline phase kicks in, powered by the slower ^{56}Ni decay chain (Shen *et al.* 2010). The optical emission is expected to fade by 2 magnitudes after $\sim$ 10 days. There have been a few viable .Ia candidates presented in the literature (Kasliwal *et al.* 2010; Perets *et al.* 2010; Poznanski *et al.* 2010), but we do not have enough objects to empirically constrain .Ia light curve shapes. Although the HFF14Spo light curves were somewhat fainter and faster than the expectations for a .Ia event, there is enough uncertainty about the diversity of .Ia light curves that this model

should not be dismissed on those merits alone.

10.1.3. *The Recurrence Problem*

An additional challenge for applying any SN-like transient model to explain the HFF14Spo events is the problem of the apparent recurrence. For all of these catastrophic stellar explosions we do not expect to see repeated transient events: the kilonova progenitor system is completely destroyed by the merger, and for the .Ia explosions the principal observed transient event is the last transient episode that system produces. Even if we suppose that an AM CVn system could produce repeated He shell flashes of similar luminosity, the period of recurrence would be of order 10^5 yr, making these effectively non-recurrent sources.

Thus, the only way to reconcile these cataclysmic explosion models with the two observed HFF14Spo events is to either (a) assert that the two events are two images of the same explosion, appearing to us separately only because of a gravitational lensing time delay (as was the case for the 5 images of SN Refsdal Kelly *et al.* 2015, 2016), or (b) invoke a highly serendipitous occurrence of two unrelated peculiar explosions in the same host galaxy in the same year.

To evaluate scenario (a), in which a lensing time delay causes the appearance of two separate events, we must rely on the available lens modeling. We have seen in Section 9 that none of the MACS J0416.1-2403 lens models predict an 8 month time delay between appearances in image 11.1 and 11.2. This is represented in Figure 8, where we have plotted the light curves for the two transient events, along with shaded vertical bars marking the time delay predictions of all models. To accept this time-delayed single explosion explanation for HFF14Spo, we would have to assume that a large systematic bias is similarly affecting all of the lens models. While we cannot rule out such a bias, the consistency of the lens modeling makes this scenario less tenable.

For the latter scenario of two unrelated explosions, it is difficult to assess the likelihood of such an occurrence quantitatively, as there are no measured rates of .Ia or kilonovae. In a study of very fast optical transients with the Pan-STARRS1 survey, Berger *et al.* (2013) derived a limit of $\lesssim 0.05$ Mpc^{-3} yr^{-1} for transients reaching $M \approx -14$ mag on a timescale of $\sim$1 day. This limit, though several orders of magnitude higher than the constraints on novae or SNe, is sufficient to make it exceedingly unlikely that two such transients would appear in the same galaxy in a single year. Furthermore, we have observed no other transients with similar luminosities and light curve shapes in our high-cadence surveys of 5 other Frontier Fields clusters. Indeed, all other transients detected in the core Frontier Fields survey have been fully consistent with normal SNe. Thus, we have no evidence to suggest that transients of this kind are much more common at $z \sim 1$.

10.2. *Luminous Blue Variable*

The transient sources categorized as Luminous Blue Variables (LBVs) are the result of eruptions or explosive episodes from massive stars ($> 10 M_\odot$). The class is exemplified by well-studied examples such as P Cygni and η Carinae (η Car) in the Milky Way and S Doradus (S-Dor) in the Large Magellanic Cloud (for recent overviews of the LBV class, see Smith *et al.* 2011; Kochanek *et al.* 2012). Although the association with massive stars is well established, this class is very heterogeneous and there is currently a vigorous debate over the precise nature of the progenitor pathway (Smith and Tombleson 2015; Humphreys *et al.* 2016; Smith 2016). The "Great Eruptions" of such massive stars are sometimes labeled as "SN impostors" because these most prominent transient episodes can exhibit light curves reminiscent of core collapse SNe, reaching peak absolute magnitudes of $\sim$-7 to -16 mag in optical bands, and lasting for tens to hundreds of days. In some cases the LBV progenitor does indeed culminate with a final true core collapse SN event (Mauerhan *et al.* 2013; Tartaglia *et al.* 2016, e.g.)

Although most giant LBV eruptions have been observed to last much longer than the HFF14Spo events (Smith *et al.* 2011), some LBVs have exhibited repeated rapid outbursts that are broadly consistent with the very fast HFF14Spo light curves. Because of this commonly seen stochastic variability, the LBV scenario does not have any trouble accounting for the HFF14Spo events as two separate episodes.

Two well-studied LBVs in particular provide a plausible match to the observed HFF14Spo events. The first is the transient "SN 2009ip" (Maza *et al.* 2009) which was later re-classified as an LBV as it showed repeated brief transient episodes (e.g., Miller *et al.* 2009; Li *et al.* 2009; Berger *et al.* 2009; Drake *et al.* 2010). Pre-eruption HST imaging demonstrated that the progenitor of SN 2009ip was likely a very high mass star ($\gtrsim 50$ M$_\odot$, Smith *et al.* 2010; Foley *et al.* 2011). Remarkably, this star eventually did explode as a true SN event, observed in 2012 (Mauerhan *et al.* 2013; Pastorello *et al.* 2013; Prieto *et al.* 2013).

The second useful comparison object is NGC3432-LBV1 (also called SN 2000ch), which was first observed as a bright variable star (Papenkova and Li 2000) and later definitively classified as an LBV (Wagner *et al.* 2004). This event exhibited at least three significant outbursts over 2-year period, which were observed in a concerted monitoring campaign (Pastorello *et al.* 2010). The spectral characteristics of this LBV suggest a similarity to Wolf-Rayet stars (Pastorello *et al.* 2010) and the variation of the SED suggests modulated dusty wind (Wagner *et al.* 2004; Kochanek *et al.* 2012). The observed sequence of erratic transient episodes may also be indicative of binary interactions similar to S-Dor (Pastorello *et al.* 2010; Smith *et al.* 2011).

Figure 11 presents a direct comparison of the observed HFF14Spo light curves against the light curves of these two rapid-eruption LBVs, SN 2009ip and NGC3432-LBV1. The brief outbursts of these LBVs have been less finely sampled than the two HFF14Spo events, but the available data show a wide variety of rise and decline times, even for a single object over a relatively narrow time window of a few months. For each of the rapid LBV outbursts shown in Figure 11 we have measured the peak luminosity and the decline time, allowing these events to be plotted in the $L_{\rm pk}$ vs. t_2 space of Figure 3 (as orange diamonds). All of the rapid LBV eruptions of SN 2009ip and NGC3432-LBV1 provide only upper limits on t_2, due to the relatively sparse photometric sampling. The observations of both HFF14Spo events are consistent with the observed luminosities and decline times of the fastest and brightest of rapid LBV outbursts.

In addition to the relatively short and very bright giant eruptions shown in Figure 11, most LBVs also commonly exhibit a slower underlying variability that has not been observed at the HFF14Spo locations. P Cygni and η Car, for example, slowly rose and fell in brightness by ∼1 to 2 mag over a timespan of several years before and after their historic giant eruptions. Such variation has not been detected at the HFF14Spo locations, as can be seen from the wide views of the HFF14Spo light curves in Figure 8. Nevertheless, given the broad range of light curve behaviors seen in LBV events, we can not reject this class as a possible explanation for the HFF14Spo system.

TODO: Measure this more quantitatively: forced photometry in drz (not diff) images at all epochs, estimate what would be the magnitude of a quiescent eta-Car-like star, and would we be able to detect a 1-2 mag brightening over the span of the HFF campaign

10.2.1. *Physical Implications of the LBV Model*

Considering the population of LBVs, the observed HFF14Spo events would stand out as extreme events. The observed rise and decline times for HFF14Spo would place both among the most rapid LBV eruptions ever seen. The peak luminosities of both HFF14Spo-1 and HFF14Spo-2 are similar to the observed luminosities of rapid, bright outbursts seen in LBVs such as SN 2009ip and NGC3432-LBV1. However, the upper edge of the range of plausible peak luminosities for both HFF14Spo events reaches 10^{42} erg s^{-1}, which would be an order of magnitude more luminous than any rapid outburst from those two nearby LBVs.

The precise physical mechanism for LBV outbursts is still not fully understood. LBV stars such as η Carshow clear evidence of ejected shells of gas, and very massive stars are known to undergo extensive mass loss as they evolve toward eventual explosion as a SN. This has led to the canonical model of LBV transient events as being the optical signature of an eruptive mass loss episode. Such mass loss could arise from a variety of direct mechanisms, such as continuum-driven super-Eddington winds (Smith and Owocki 2006), pulsational pair instability ejections (Woosley *et al.* 2007), and shock heating of stellar envelopes from internal shell-burning instabilities (Dessart *et al.* 2010). This is far from an exhaustive list, and none of these explanations are entirely sufficient to account for all of the observed diversity of LBV behaviors or the structural complexity the most well-studied LBVs (e.g. Smith *et al.* 2011; Kochanek *et al.* 2012).

Although we do not have a complete physical model in hand, we can nevertheless explore some of the physical implications of an LBV classification for the two HFF14Spo events. We first make a rough estimate of the total radiated energy, which can be computed using the decline timescale t_2 and the peak luminosity $L_{\rm pk}$ following Smith *et al.* (2011):

$$E_{\rm rad} = \zeta t_2 L_{\rm pk}, \tag{3}$$

where ζ is a factor of order unity that depends on the precise shape of the light curve.[8] Adopting $L_{\rm pk} \sim 10^{41}$ erg s^{-1} and t_2 ∼2 days (as shown in Figure 3), we find that the total radiated energy isi $E_{\rm rad} \sim 10^{46}$ erg. A realistic range for this estimate would span $10^{44} < E_{\rm rad} < 10^{47}$ erg, due to uncertainties in the magnification, bolometric luminosity correction, decline time, and light curve shape (in roughly that order of importance). These uncertainties notwithstanding, our crude estimate does fall well within the range of plausible values for the total radiated energy of a major LBV outburst.

If LBV eruptions are driven by significant mass ejection events, then the energy budget would also include a substantial amount of kinetic energy imparted to the ejected gas shell. Without spectroscopic information from the HFF14Spo transients we can not place any realistic estimate on the kinetic energy. Nevertheless, we can take the radiated energy as a rough lower limit on the total energy release and ask what timescale would be required for a massive star to build up that amount of energy. This approach assumes that the energy released in an LBV eruption is generated slowly in the stellar interior and is in some way "bottled up" by the stellar envelope, before being released in a rapid mass ejection. The "build-up" timescale to match the radiative energy release is then

$$t_{\rm rad} = \frac{E_{\rm rad}}{L_{\rm qui}} = t_2 \frac{\xi L_{\rm pk}}{L_{\rm qui}}, \tag{4}$$

where $L_{\rm qui}$ is the luminosity of the LBV progenitor star during quiescence. For the HFF14Spo events we have no useful constraint on the quiescent luminosity, but for evaluating the LBV scenario we can assume it is similar to the local LBVs whose progenitors have been directly observed. This gives a range for the radiative build-up timescale between $t_{\rm rad} \sim 30$ days if the progenitor is η Car-like ($M_V \sim -12$), or $t_{\rm rad} \sim 20$ years if it is similar to the faintest known LBV progenitors (e.g. SN 2010dn, with $M_V \sim -6$).

Alternatively, a more informative approach is to assert that the build-up timescale for HFF14Spo corresponds to the observed rest-frame lag between the two events, roughly 120 days. Adopting $L_{\rm pk} = 10^{41}$ erg s^{-1} and $t_2 =$ 2 days, if we assume $t_{\rm rad} = 120$ days we can infer that the quiescent luminosity of the HFF14Spo progenitor would be $L_{\rm qui} \sim 10^{39.5}$ erg s−1 ($M_V \sim -10$). This is a very reasonable quiescent luminosity value for the massive ($>$ 10M$_\odot$) progenitor stars expected for LBVs.

Although the above discussion shows that the observations of the HFF14Spo transients are largely consistent with the observed characteristics of known LBV systems, this does not mean that we have a viable physical model to explain these events. Rapid transient episodes in LBVs such as SN 2002kg and SN 2009ip may best be explained by a sudden ejection of an optically thick shell (e.g., Smith *et al.* 2010, 2011), or by some form of S Dor-type variability (Weis and Bomans 2005; Van Dyk *et al.* 2006; Foley *et al.* 2011), which may be driven by stellar pulsation rather than mass ejection (van Genderen *et al.* 1997; van Genderen 2001).

For massive stars such as η Carat its great eruption and the rapidly varying SN 2009ip, the effective photospheric radius during eruption must have been comparable to the orbit of Saturn (10^{14} cm; Davidson and Humphreys 1997; Smith *et al.* 2011; Foley *et al.* 2011). With observed photospheric velocities of order 500 km s^{-1} for such events,

[8] Note that Smith *et al.* (2011) used $t_{1.5}$ instead of t_2, which amounts to a different light curve shape term, ζ.

the dynamical timescale of the extended photosphere is on the order of tens to hundreds of days. Thus, if the very rapid light curves of both HFF14Spo events are indeed LBV eruptions, then they will be near the extreme limits of physical models for massive stellar eruptions.

10.3. *Recurrent Nova*

Novae are represented in Figure **??** as a grey band, which traces the maximum magnitude - rate of decline (MMRD) relation. Nova explosions occur in binary star systems in which the more massive star is a white dwarf that accretes matter from its companion, which may be a main sequence dwarf or evolved giant star overfilling its Roche Lobe. The white dwarf builds up a dense layer of H-rich material on its surface until the high pressure and temperature triggers nuclear fusion, resulting in a surface explosion that causes the white dwarf to brighten by several orders of magnitude, but does not completely disrupt the star. In a recurrent nova (RN) system, the mass transfer from the companion to the white dwarf restarts after the explosion, so the cycle may begin again and repeat after a period of months or years.

The seminal work of Zwicky (1936) and McLaughlin (1939) first showed that more luminous novae within the Milky Way tend to have more rapidly declining light curves, which is now the basis of the maximum-magnitude versus rate-of-decline (MMRD) relationship. The basic form of the MMRD relation has been theoretically attributed to a dependence of the peak luminosity on the mass of the accreting white dwarf (e.g. Livio 1992). Studies of extragalactic novae reaching as far as the Virgo cluster have shown that the MMRD relation is broadly applicable to all nova populations, though with significant scatter (e.g. Ciardullo *et al.* 1990; Della Valle and Livio 1995; Ferrarese *et al.* 2003; Shafter *et al.* 2011). Amidst that scatter, there may also be sub-populations of novae that deviate from the traditional MMRD form (Kasliwal *et al.* 2011b), and recurrent novae (RNe) in particular may be poorly represented by the MMRD (Shafter *et al.* 2011; Hachisu and Kato 2015)

In Figure **??**, the dark grey region follows the empirical constraints on the MMRD from Della Valle and Livio (1995), and the wider light grey band allows for the increased scatter about that relation that has been noted from more extensive surveys of novae in the Milky Way (Downes and Duerbeck 2000), M31 (Shafter *et al.* 2011) and elsewhere in the local group (Kasliwal *et al.* 2011b). Nova outbursts can exhibit decline times from $\sim$1 day to many months, so the timescale of the HFF14Spo light curves can easily be accommodated by the nova scenario. However, the peak luminosities inferred for the HFF14Spo events are larger than any known novae, perhaps by as much as 2 orders of magnitude.

Figure 3 shows a narrower slice of the same phase space as in Figure **??**, zooming in on the "fast and faint" region from the lower left corner. The observed constraints from the two published kilonova candidates are shown, which provide only lower limits on the peak luminosity (Tanvir *et al.* 2013), or the decline timescale (Perley *et al.* 2009). Two .Ia candidates are also plotted, SN 2002bj (Poznanski *et al.* 2010) and SN 2010X (Kasliwal *et al.* 2010). The sample of observed nova outbursts (shown as solid points) demonstrates the observed scatter about the MMRD relation.

One primary line of evidence supporting the nova hypothesis comes from the HFF14Spo light curves. Many RN light curves are similar in shape to the HFF14Spo episodes, exhibiting a sharp rise ($<$ 10 days in the rest-frame) and a similarly rapid decline. Figure 10 compares the HFF14Spo light curves to template light curves from RNe within our galaxy and in M31. There are 10 known RNe in the Milky Way galaxy, and 7 of these exhibit outbursts that decline rapidly, fading by 2 magnitudes in less than 10 days (Schaefer 2010) The gray shaded region in Figure 10 encompasses the V band light curve templates for all 7 of these events, from Schaefer (2010). The Andromeda galaxy (M31) also hosts at least one RN with a rapidly declining light curve. The 2014 eruption of this well-studied nova, M31N 2008a-12, is shown as a solid black line in Figure 10, fading by 2 mags in less than 3 days. This comparison demonstrates that the sudden disappearance of both of the HFF14Spo transient events is fully consistent with the eruptions of known RNe in the local universe.

The rise time of the HFF14Spo events is somewhat out of the ordinary for nova outbursts. In particular, for recurrent nova eruptions that decline rapidly ($t_2 < 10$ days) they tend to also reach peak brightness very quickly, on timescales < 1 day (Schaefer 2010). The 2014 eruption of the rapid-recurrence nova M31N 2008a-12 reached maximum brightness in a little under 1 day (Darnley *et al.* 2015). However, the rise time for nova eruptions is poorly constrained, as rapid-cadence imaging is rarely secured until after an initial detection near peak brightness. Unlike the situation with a kilonova light curve, there is no a priori physical expectation for an especially rapid rise to peak in nova light curves.

Among the most luminous classical novae known, a similarly rapid decline time is not unheard of. For example, the bright nova M31N-2007-11d had $t_2 = 9.5$ days (Shafter *et al.* 2009). The extremely luminous nova SN 2010U had $t_2 = 3.5 \pm 0.3$ (Czekala *et al.* 2013). The nova L91 required at least 4 days to rise to maximum (Shafter *et al.* 2009), and then declined with $t_2 = 6 \pm 1$ days (della Valle 1991; Williams *et al.* 1994; Schwarz *et al.* 2001).

Another reason to consider the RN model is that it provides a natural explanation for having two separate explosions that are coincident in space but not in time. If HFF14Spo is a RN, then the two observed episodes can be attributed to two distinct nova eruptions, and the gravitational lensing time delay does not need to match the observed 8 month separation between the January and August 2014 appearances.

Although *qualitatively* consistent with the 8-month separation, the RN model is strained by a quantitative assessment of the recurrence period. If HFF14Spo is indeed a RN at $z = 1$, then the recurrence timescale in the rest-frame is 120 ± 30 days ($3 - 5$ months), where the uncertainty accounts for the 1σ range of modeled gravitational lensing time delays. This would be a singularly rapid recurrence period, significantly faster than all 11 RNe in our own galaxy, which have recurrence timescales ranging from 15 years (RS Oph) to 80 years (T CrB). For the 5 galactic RNe with a rapidly declining outburst light curve (U Sco, V2487 Oph, V394 CrA, T CrB, and V745 Sco), the median recurrence timescale is 21 years. The fastest measured recurrence timescale belongs to the Andromeda galaxy nova M31N 2008a-12,

which has exhibited a new outburst every year from 2009-2015 (Tang *et al.* 2014; Darnley *et al.* 2014, 2015; Henze *et al.* 2015a,b). Although this M31 record-holder demonstrates that very rapid recurrence is possible, classifying HFF14Spo as a RN would still require a very extreme mass transfer rate to accommodate the < 1 year recurrence.

Another major concern with the RN hypothesis for HFF14Spo is apparent in Figure 3, which shows that the two HFF14Spo events are substantially brighter than all known novae – perhaps by as much as 2 orders of magnitude. One might attempt to reconcile the HFF14Spo luminosity more comfortably with the nova class by assuming a significant lensing magnification for one of the two events. This would drive down the intrinsic luminosity, perhaps to $\sim 10^{40}$ erg s$-$1, on the edge of the nova region. However, this assumption implicitly moves the lensing critical curve to be closer to the HFF14Spo event in question. That pulls the critical curve away from the other HFF14Spo position, which makes that second event *more inconsistent* with observed nova peak luminosities.

10.3.1. *Physical Implications of the RN Model*

The physical limits of the RN model are best evaluated by combining the two key observables of recurrence period and peak brightness. In this examination we rely on a pair of papers that evaluated an extensive grid of nova models through multiple cycles of outburst and quiescence (Prialnik and Kovetz 1995; Yaron *et al.* 2005). Figure 12 plots first the RN outburst amplitude (the apparent magnitude between outbursts minus the apparent magnitude at peak) and then the peak luminosity against the log of the recurrence period in years. For the HFF14Spo events we can only measure a lower limit on the outburst amplitude, since the presumed progenitor star is unresolved, so no measurement is available at quiescence. Figure 12 shows that a recurrence period as fast as one year is expected only for a RN system in which the primary WD is both very close to the Chandrasekhar mass limit (1.4 $M_\odot$) and also has an extraordinarily rapid mass transfer rate ($\sim 10^{-6}$ $M_\odot$ yr^{-1}). The models of Yaron *et al.* (2005) suggest that such systems should have a very low peak amplitude (barely consistent with the lower limit for HFF14Spo) and a low peak luminosity ($\sim$100 times less luminous than the HFF14Spo events).

The closest analog for the HFF14Spo events from the population of known RN systems is the nova M31N 2008a-12. Kato *et al.* (2015) provided a theoretical model that can account for the key observational characteristics of this remarkable nova: the very rapid recurrence timescale ($<$1 yr), fast optical light curve ($t_2 \sim 2$ days), and short supersoft x-ray phase (6-18 days after optical outburst Henze *et al.* 2015b). To match these observations, Kato *et al.* invoke a 1.38 $M_\odot$ white dwarf primary, drawing mass from a companion at a rate of 1.6×10^{-7} $M_\odot$ yr^{-1}. This is largely consistent with the theoretical expectations derived by Yaron *et al.* (2005), and reinforces the conclusion that a combination of a high mass white dwarf and efficient mass transfer are the key ingredients for rapid recurrence and short light curves. The one feature that can not be effectively explained with this scenario is the peculiarly high luminosity of the HFF14Spo events – even after accounting for the very large uncertainties. If the HFF14Spo transients are caused by a single RN system, then that progenitor system would be the most extreme WD binary yet known.

11. NON-EXPLOSIVE ASTROPHYSICAL TRANSIENTS

There are several categories of astrophysical transients that are not related to stellar explosions, and we find that these models cannot accommodate the observations of the HFF14Spo transients. We may first dismiss any of the category of *periodic* sources (e.g. Cepheids, RR Lyrae, or Mira variables) that exhibit regular changes in flux due to pulsations of the stellar photosphere. These variable stars do not exhibit sharp, isolated transient episodes that could match the HFF14Spo light curve shapes.

We can also rule out active galactic nuclei (AGN), in which brief transient episodes (a few days in duration) may be observed from X-ray to infrared wavelengths (e.g. Gaskell and Klimek 2003). The AGN hypothesis for HFF14Spo is disfavored for three primary reasons: First, AGN that exhibit short-duration transient events also typically exhibit slower variation on much longer timescales, which is not observed at either of the HFF14Spo locations. Second, the spectrum of the HFF14Spo host galaxy shows none of the broad emission lines that are often (though not always) observed in AGN. Third, an AGN would necessarily be located at the center of the host galaxy. In Section 8 we saw that there are minor differences in the host galaxy properties (i.e. rest-frame U-V color and mean stellar age) from the HFF14Spo-1 and HFF14Spo-2 locations to the center of the host galaxy at image 11.3 Although by no means definitive, this suggests that the HFF14Spo events were not located at the physical center of the host galaxy, and therefore are not related to an AGN. **TODO:** Update with MUSE results

Stellar flares provide a third very common source for optical transient events. Relatively mild stellar flares may be caused by magnetic activity in the stellar atmosphere, and the brightest flare events (so-called "superflares") may be generated by perturbations to the stellar atmosphere via interactions from a disk, a binary companion, or a planet. In these circumstances the stars release a *total* energy in the range of 10^{33} to 10^{38} erg over a span of minutes to hours (Balona 2012; Karoff *et al.* 2016). This falls far short of the observed energy release from the HFF14Spo transients, so we can also dismiss stellar flares as implausible for this source.

11.1. *Microlensing*

In the presence of strong gravitational lensing it is possible to generate a transient event from lensing effects alone. In this case the background source has a steady luminosity but the relative motion of the source, lens, and observer causes the magnification of that source to change rapidly with time.

A commonly observed example is the microlensing of a bright background source (a quasar) by a galaxy-scale lens (Wambsganss 2001; Kochanek 2004). In this optically thick microlensing regime, the lensing potential

along the line of sight to the quasar is composed of many stellar-mass objects. Each compact object along the line of sight generates a separate critical lensing curve, resulting in a complex web of overlapping critical curves. As all of these lensing stars are in motion relative to the background source, the web of caustics will shift across the source position, leading to a stochastic variability on timescales of months to years. This scenario is inconsistent with the observed data, as the two HFF14Spo events were far too short in duration and did not exhibit the repeated "flickering" variation that would be expected from optically thick microlensing.

A second possibility is through an isolated strong lensing event with a rapid timescale, such as a background star crossing over a lensing critical curve. This corresponds to the optically thin microlensing regime, and is similar to the "local" microlensing light curves observed when stars within our galaxy or neighboring dwarf galaxies pass behind a massive compact halo object (Paczynski 1986; Alcock *et al.* 1993; Aubourg *et al.* 1993; Udalski *et al.* 1993). In the case of a star crossing the caustic of a smooth lensing potential, the amplification of the source flux would increase (decrease) with a characteristic $t^{-1/2}$ profile as it moves toward (away from) the caustic. This slowly evolving light curve transitions to a very sharp decline (rise) when the star has moved to the other side of the caustic (Schneider and Weiss 1986; MiraldaEscude 1991). With a more complex lens comprising many compact objects, the light curve would exhibit a superposition of many such sharp peaks (Lewis *et al.* 1993).

To generate an isolated microlensing event, the background source would have to be the dominant source of luminosity in its environment, meaning it must be a very bright O or B star with mass of order 10 $M_\odot$. Depending on its age, the size of such a star would range from a few to a few dozen times the size of the sun. The net relative transverse velocity would be on the order of a few 100 km/s, which is comparable to the orbital velocity of stars within a galaxy or galaxies within a cluster. In the case of a smooth cluster potential—the characteristic timescale of such an event would be on the order of hours or days Chang and Refsdal (1979, 1984); MiraldaEscude (1991), which is in the vicinity of the timescales observed for the HFF14Spo events. However, if we apply this scenario to the MACS J0416.1-2403 field, we can not plausibly generate two events with similar decay timescales at distinct locations on the sky. This is because a caustic-crossing transient event must necessarily appear at the location of the lensing critical curve, but in this case the critical curve most likely passes between the two observed HFF14Spo locations. At best, a caustic crossing could account for only one of the HFF14Spo events, not both.

REFERENCES

P. L. Kelly, S. A. Rodney, T. Treu, R. J. Foley, G. Brammer, K. B. Schmidt, A. Zitrin, A. Sonnenfeld, L.-G. Strolger, O. Graur, A. V. Filippenko, S. W. Jha, A. G. Riess, M. Bradac, B. J. Weiner, D. Scolnic, M. A. Malkan, A. von der Linden, M. Trenti, J. Hjorth, R. Gavazzi, A. Fontana, J. C. Merten, C. McCully, T. Jones, M. Postman, A. Dressler, B. Patel, S. B. Cenko, M. L. Graham, and B. E. Tucker, Science **347**, 1123 (2015).

S. A. Rodney, B. Patel, D. Scolnic, R. J. Foley, A. Molino, G. Brammer, M. Jauzac, M. Bradac, D. Coe, T. Broadhurst, J. M. Diego, O. Graur, J. Hjorth, A. Hoag, S. W. Jha, T. L. Johnson, P. Kelly, D. Lam, C. McCully, E. Medezinski, M. Meneghetti, J. Merten, J. Richard, A. Riess, K. Sharon, L.-G. Strolger, T. Treu, X. Wang, L. L. R. Williams, and A. Zitrin, ApJ, in press (2015).

M. M. Kasliwal, S. R. Kulkarni, A. Gal-Yam, O. Yaron, R. M. Quimby, E. O. Ofek, P. Nugent, D. Poznanski, J. Jacobsen, A. Sternberg, I. Arcavi, D. A. Howell, M. Sullivan, D. J. Rich, P. F. Burke, J. Brimacombe, D. Milisavljevic, R. Fesen, L. Bildsten, K. Shen, S. B. Cenko, J. S. Bloom, E. Hsiao, N. M. Law, N. Gehrels, S. Immler, R. Dekany, G. Rahmer, D. Hale, R. Smith, J. Zolkower, V. Velur, R. Walters, J. Henning, K. Bui, and D. McKenna, ApJ **723**, L98 (2010).

M. M. Phillips, ApJ **413**, L105 (1993).

A. Gal-Yam, Science **337**, 927 (2012).

I. Arcavi, W. M. Wolf, D. A. Howell, L. Bildsten, G. Leloudas, D. Hardin, S. Prajs, D. A. Perley, G. Svirski, A. Gal-Yam, B. Katz, C. McCully, S. B. Cenko, C. Lidman, M. Sullivan, S. Valenti, P. Astier, C. Balland, R. G. Carlberg, A. Conley, D. Fouchez, J. Guy, R. Pain, N. Palanque-Delabrouille, K. Perrett, C. J. Pritchet, N. Regnault, J. Rich, and V. Ruhlmann-Kleider, ApJ **819**, 35 (2016).

R. J. Foley, P. J. Challis, R. Chornock, M. Ganeshalingam, W. Li, G. H. Marion, N. I. Morrell, G. Pignata, M. D. Stritzinger, J. M. Silverman, X. Wang, J. P. Anderson, A. V. Filippenko, W. L. Freedman, M. Hamuy, S. W. Jha, R. P. Kirshner, C. McCully, S. E. Persson, M. M. Phillips, D. E. Reichart, and A. M. Soderberg, ApJ **767**, 57 (2013).

M. R. Drout, R. Chornock, A. M. Soderberg, N. E. Sanders, R. McKinnon, A. Rest, R. J. Foley, D. Milisavljevic, R. Margutti, E. Berger, M. Calkins, W. Fong, S. Gezari, M. E. Huber, E. Kankare, R. P. Kirshner, C. Leibler, R. Lunnan, S. Mattila, G. H. Marion, G. Narayan, A. G. Riess, K. C. Roth, D. Scolnic, S. J. Smartt, J. L. Tonry, W. S. Burgett, K. C. Chambers, K. W. Hodapp, R. Jedicke, N. Kaiser, E. A. Magnier, N. Metcalfe, J. S. Morgan, P. A. Price, and C. Waters, ApJ **794**, 23 (2014).

A. V. Filippenko, R. Chornock, B. Swift, M. Modjaz, R. Simcoe, and M. Rauch, IAU Circ. **8159** (2003).

H. B. Perets, C. Badenes, I. Arcavi, J. D. Simon, and A. Gal-yam, ApJ **730**, 89 (2011).

M. M. Kasliwal, S. R. Kulkarni, A. Gal-Yam, P. E. Nugent, M. Sullivan, L. Bildsten, O. Yaron, H. B. Perets, I. Arcavi, S. Ben-Ami, V. B. Bhalerao, J. S. Bloom, S. B. Cenko, A. V. Filippenko, D. A. Frail, M. Ganeshalingam, A. Horesh, D. A. Howell, N. M. Law, D. C. Leonard, W. Li, E. O. Ofek, D. Polishook, D. Poznanski, R. M. Quimby, J. M. Silverman, A. Sternberg, and D. Xu, ApJ **755**, 161 (2012).

U. Munari, A. Henden, S. Kiyota, D. Laney, F. Marang, T. Zwitter, R. L. M. Corradi, S. Desidera, P. M. Marrese, E. Giro, F. Boschi, and M. B. Schwartz, A&A **389**, L51 (2002).

S. R. Kulkarni, E. O. Ofek, A. Rau, S. B. Cenko, A. M. Soderberg, D. B. Fox, A. Gal-Yam, P. L. Capak, D. S. Moon, W. Li, A. V. Filippenko, E. Egami, J. Kartaltepe, and D. B. Sanders, Nature **447**, 458 (2007).

M. M. Kasliwal, S. R. Kulkarni, I. Arcavi, R. M. Quimby, E. O. Ofek, P. Nugent, J. Jacobsen, A. Gal-Yam, Y. Green, O. Yaron, D. B. Fox, J. L. Howell, S. B. Cenko, I. Kleiser, J. S. Bloom, A. Miller, W. Li, A. V. Filippenko, D. Starr, D. Poznanski, N. M. Law, G. Helou, D. A. Frail, J. D. Neill, K. Forster, D. C. Martin, S. P. Tendulkar, N. Gehrels, J. Kennea, M. Sullivan, L. Bildsten, R. Dekany, G. Rahmer, D. Hale, R. Smith, J. Zolkower, V. Velur, R. Walters, J. Henning, K. Bui, D. McKenna, and C. Blake, ApJ **730**, 134 (2011a).

L.-X. Li and B. Paczyński, ApJ **507**, L59 (1998).

S. R. Kulkarni, ArXiv Astrophysics e-prints (2005).

D. A. Perley, B. D. Metzger, J. Granot, N. R. Butler, T. Sakamoto, E. Ramirez-Ruiz, A. J. Levan, J. S. Bloom, A. A. Miller, A. Bunker, H.-W. Chen, A. V. Filippenko, N. Gehrels, K. Glazebrook, P. B. Hall, K. C. Hurley, D. Kocevski, W. Li, S. Lopez, J. Norris, A. L. Piro, D. Poznanski, J. X. Prochaska, E. Quataert, and N. Tanvir, ApJ **696**, 1871 (2009).

N. R. Tanvir, A. J. Levan, A. S. Fruchter, J. Hjorth, R. A. Hounsell, K. Wiersema, and R. L. Tunnicliffe, Nature **500**, 547 (2013).

B. D. Metzger, G. Martínez-Pinedo, S. Darbha, E. Quataert, A. Arcones, D. Kasen, R. Thomas, P. Nugent, I. V. Panov, and N. T. Zinner, MNRAS **406**, 2650 (2010).

J. Barnes and D. Kasen, ApJ **775**, 18 (2013).

D. Kasen, R. Fernández, and B. D. Metzger, MNRAS **450**, 1777 (2015).

L. Bildsten, K. J. Shen, N. N. Weinberg, and G. Nelemans, ApJ **662**, L95 (2007).

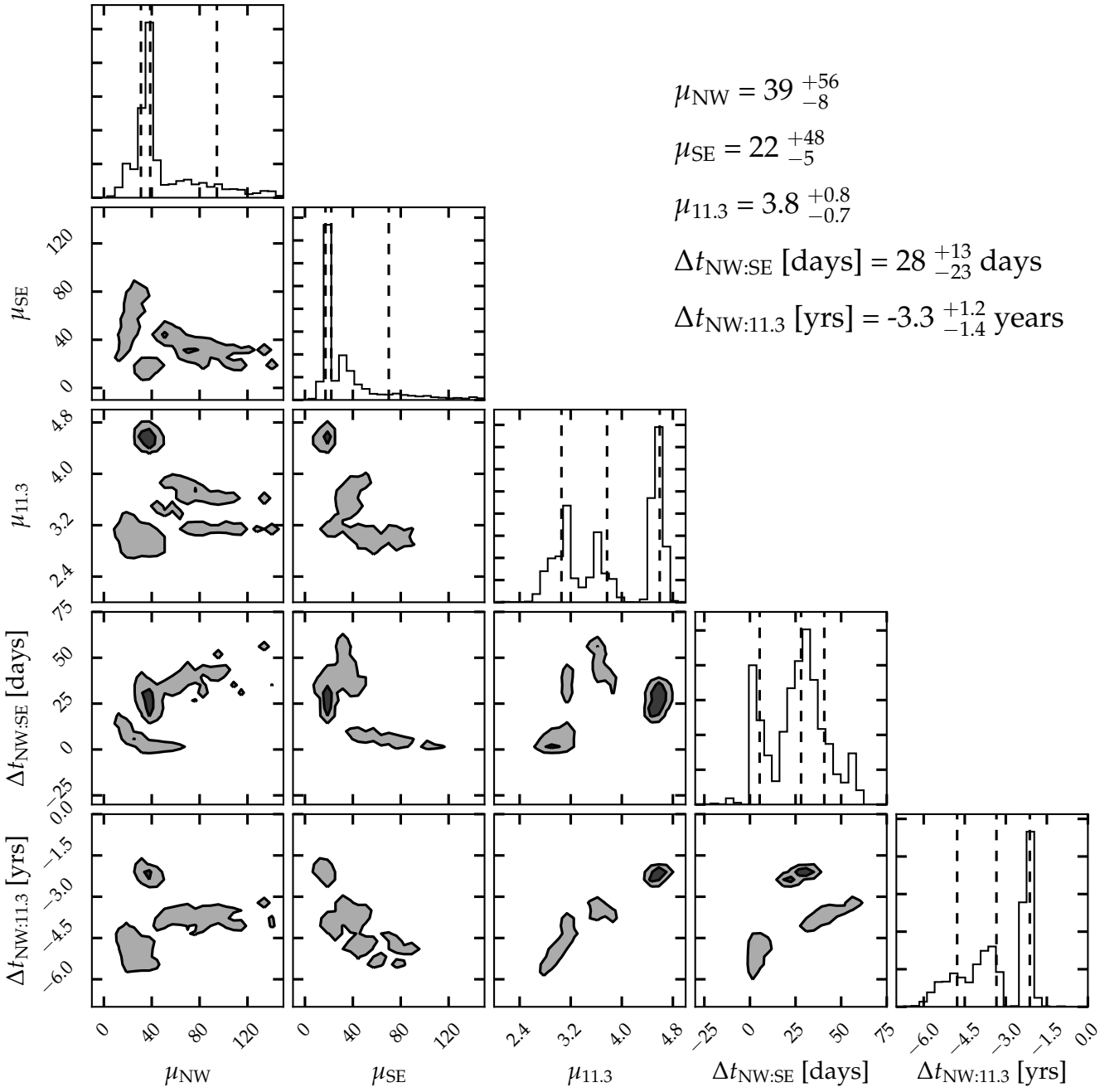

FIG. 9.— Probability distributions for the five primary magnification and time delay observables, drawn from a combination of results from four lens models. Contours shown in the ten panels at the lower left mark the 1-σ and 2-σ confidence regions in each 2D slice of the parameter space. Histograms at the top of each column show the marginalized 1D probability distributions, with dashed vertical lines marking the mean and 1σ confidence region. These mean values and uncertainties are also reported in the table of values at the upper right.

B. Warner, Ap&SS **225**, 249 (1995).
G. Nelemans and C. A. Tout, MNRAS **356**, 753 (2005).
K. Nomoto, ApJ **253**, 798 (1982a).
K. Nomoto, ApJ **257**, 780 (1982b).
S. E. Woosley and T. A. Weaver, ARA&A **24**, 205 (1986).
S. E. Woosley and T. A. Weaver, ApJ **423**, 371 (1994).
K. J. Shen, D. Kasen, N. N. Weinberg, L. Bildsten, and E. Scannapieco, ApJ **715**, 767 (2010).
H. B. Perets, A. Gal-Yam, P. A. Mazzali, D. Arnett, D. Kagan, A. V. Filippenko, W. Li, I. Arcavi, S. B. Cenko, D. B. Fox, D. C. Leonard, D.-S. Moon, D. J. Sand, A. M. Soderberg, J. P. Anderson, P. A. James, R. J. Foley, M. Ganeshalingam, E. O. Ofek, L. Bildsten, G. Nelemans, K. J. Shen, N. N. Weinberg, B. D. Metzger, A. L. Piro, E. Quataert, M. Kiewe, and D. Poznanski, Nature **465**, 322 (2010).
D. Poznanski, R. Chornock, P. E. Nugent, J. S. Bloom, A. V. Filippenko, M. Ganeshalingam, D. C. Leonard, W. Li, and R. C. Thomas, Science **327**, 58 (2010).

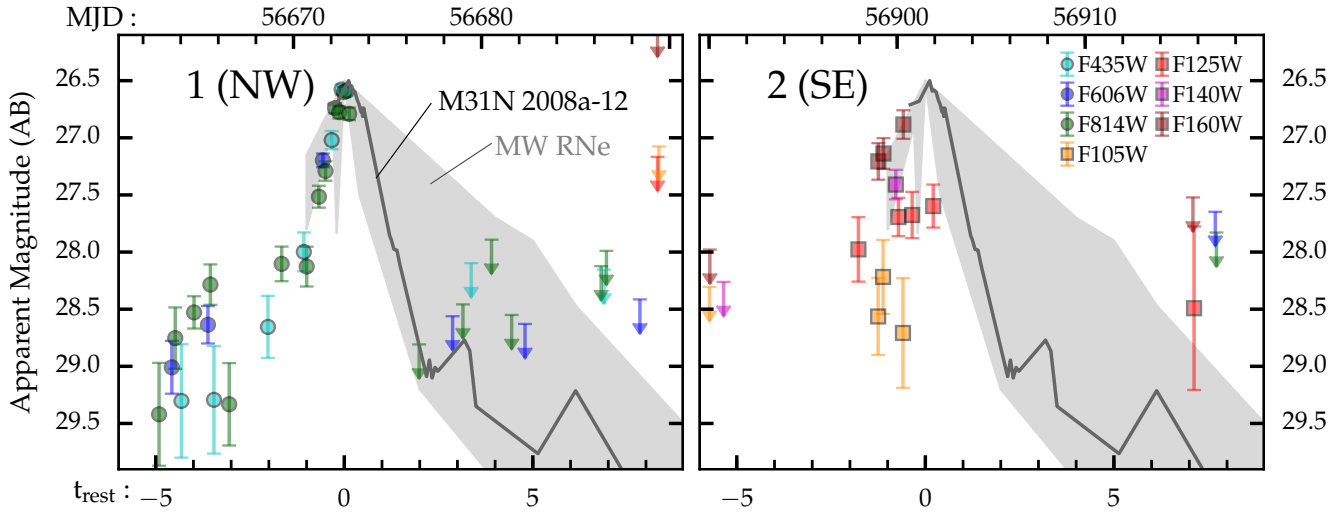

FIG. 10.— Comparison of the HFF14Spo light curves against template light curves for RN outbursts. Colored markers show the HFF14Spo light curve data, as in Figure 2, plotting the apparent magnitude as a function of time in the rest frame (bottom axis) and observer frame (top axis). The gray shaded regions encompass the outburst light curve shapes of 5 of the 11 known galactic RNe (U Sco, V2487 Oph, V394 CrA, T CrB, and V745 Sco), selected because they exhibit a rapid decline in their light curves (Schaefer 2010). The solid black line traces the 2014 outburst light curve shape for the rapid-recurrence nova M31N 2008a-12 (Darnley *et al.* 2014). All template light curves have been normalized to match the observed peaks of the HFF14Spo events.

P. L. Kelly, S. A. Rodney, T. Treu, L.-G. Strolger, R. J. Foley, S. W. Jha, J. Selsing, G. Brammer, M. Bradač, S. B. Cenko, O. Graur, A. V. Filippenko, J. Hjorth, C. McCully, A. Molino, M. Nonino, A. G. Riess, K. B. Schmidt, B. Tucker, A. von der Linden, B. J. Weiner, and A. Zitrin, ApJ **819**, L8 (2016).

E. Berger, C. N. Leibler, R. Chornock, A. Rest, R. J. Foley, A. M. Soderberg, P. A. Price, W. S. Burgett, K. C. Chambers, H. Flewelling, M. E. Huber, E. A. Magnier, N. Metcalfe, C. W. Stubbs, and J. L. Tonry, ApJ **779**, 18 (2013).

N. Smith, W. Li, J. M. Silverman, M. Ganeshalingam, and A. V. Filippenko, MNRAS **415**, 773 (2011).

C. S. Kochanek, D. M. Szczygieł, and K. Z. Stanek, ApJ **758**, 142 (2012).

N. Smith and R. Tombleson, MNRAS **447**, 598 (2015).

R. M. Humphreys, K. Weis, K. Davidson, and M. S. Gordon, ApJ **825**, 64 (2016).

N. Smith, ArXiv e-prints (2016).

J. C. Mauerhan, N. Smith, A. V. Filippenko, K. B. Blanchard, P. K. Blanchard, C. F. E. Casper, S. B. Cenko, K. I. Clubb, D. P. Cohen, K. L. Fuller, G. Z. Li, and J. M. Silverman, MNRAS **430**, 1801 (2013).

L. Tartaglia, A. Pastorello, M. Sullivan, C. Baltay, D. Rabinowitz, P. Nugent, A. J. Drake, S. G. Djorgovski, A. Gal-Yam, S. Fabrika, E. A. Barsukova, V. P. Goranskij, A. F. Valeev, T. Fatkhullin, S. Schulze, A. Mehner, F. E. Bauer, S. Taubenberger, J. Nordin, S. Valenti, D. A. Howell, S. Benetti, E. Cappellaro, G. Fasano, N. Elias-Rosa, M. Barbieri, D. Bettoni, A. Harutyunyan, T. Kangas, E. Kankare, J. C. Martin, S. Mattila, A. Morales-Garoffolo, P. Ochner, U. D. Rebbapragada, G. Terreran, L. Tomasella, M. Turatto, E. Verroi, and P. R. Woźniak, MNRAS **459**, 1039 (2016).

J. Maza, M. Hamuy, R. Antezana, L. Gonzalez, P. Gonzalez, S. Lopez, G. Silva, *et al.*, CBET , 1 (2009).

A. A. Miller, W. Li, P. E. Nugent, J. S. Bloom, A. V. Filippenko, and A. T. Merritt, The Astronomer's Telegram **2183** (2009).

W. Li, N. Smith, A. A. Miller, and A. V. Filippenko, The Astronomer's Telegram **2212** (2009).

E. Berger, R. Foley, and I. Ivans, The Astronomer's Telegram **2184** (2009).

A. J. Drake, J. L. Prieto, S. G. Djorgovski, A. A. Mahabal, M. J. Graham, R. Williams, R. H. McNaught, M. Catelan, E. Christensen, E. C. Beshore, S. M. Larson, and S. Howerton, The Astronomer's Telegram **2897** (2010).

N. Smith, A. Miller, W. Li, A. V. Filippenko, J. M. Silverman, A. W. Howard, P. Nugent, G. W. Marcy, J. S. Bloom, A. M. Ghez, J. Lu, S. Yelda, R. A. Bernstein, and J. E. Colucci, AJ **139**, 1451 (2010).

R. J. Foley, E. Berger, O. Fox, E. M. Levesque, P. J. Challis, I. I. Ivans, J. E. Rhoads, and A. M. Soderberg, ApJ **732**, 32 (2011).

A. Pastorello, E. Cappellaro, C. Inserra, S. J. Smartt, G. Pignata, S. Benetti, S. Valenti, M. Fraser, K. Takáts, S. Benitez, M. T. Botticella, J. Brimacombe, F. Bufano, F. Cellier-Holzem, M. T. Costado, G. Cupani, I. Curtis, N. Elias-Rosa, M. Ergon, J. P. U. Fynbo, F.-J. Hambsch, M. Hamuy, A. Harutyunyan, K. M. Ivarson, E. Kankare, J. C. Martin, R. Kotak, A. P. LaCluyze, K. Maguire, S. Mattila, J. Maza, M. McCrum, M. Miluzio, H. U. Norgaard-Nielsen, M. C. Nysewander, P. Ochner, Y.-C. Pan, M. L. Pumo, D. E. Reichart, T. G. Tan, S. Taubenberger, L. Tomasella, M. Turatto, and D. Wright, ApJ **767**, 1 (2013).

J. L. Prieto, J. Brimacombe, A. J. Drake, and S. Howerton, ApJ **763**, L27 (2013).

M. Papenkova and W. D. Li, IAU Circ. **7415** (2000).

R. M. Wagner, F. J. Vrba, A. A. Henden, B. Canzian, C. B. Luginbuhl, A. V. Filippenko, R. Chornock, W. Li, A. L. Coil, G. D. Schmidt, P. S. Smith, S. Starrfield, S. Klose, J. Tichá, M. Tichý, J. Gorosabel, R. Hudec, and V. Simon, PASP **116**, 326 (2004).

A. Pastorello, M. T. Botticella, C. Trundle, S. Taubenberger, S. Mattila, E. Kankare, N. Elias-Rosa, S. Benetti, G. Duszanowicz, L. Hermansson, J. E. Beckman, F. Bufano, M. Fraser, A. Harutyunyan, H. Navasardyan, S. J. Smartt, S. D. van Dyk, J. S. Vink, and R. M. Wagner, MNRAS **408**, 181 (2010).

N. Smith and S. P. Owocki, ApJ **645**, L45 (2006).

S. E. Woosley, D. Kasen, S. Blinnikov, and E. Sorokina, ApJ **662**, 487 (2007).

L. Dessart, E. Livne, and R. Waldman, MNRAS **405**, 2113 (2010).

K. Weis and D. J. Bomans, A&A **429**, L13 (2005).

S. D. Van Dyk, W. Li, A. V. Filippenko, R. M. Humphreys, R. Chornock, R. Foley, and P. M. Challis, ArXiv Astrophysics e-prints (2006).

A. M. van Genderen, M. de Groot, and C. Sterken, A&AS **124** (1997).

A. M. van Genderen, A&A **366**, 508 (2001).

K. Davidson and R. M. Humphreys, ARA&A **35**, 1 (1997).

F. Zwicky, PASP **48**, 191 (1936).

D. B. McLaughlin, Popular Astronomy **47**, 410 (1939).

M. Livio, ApJ **393**, 516 (1992).

R. Ciardullo, P. Tamblyn, G. H. Jacoby, H. C. Ford, and R. E. Williams, AJ **99**, 1079 (1990).

M. Della Valle and M. Livio, ApJ **452**, 704 (1995).

L. Ferrarese, P. Côté, and A. Jordán, ApJ **599**, 1302 (2003).

A. W. Shafter, M. J. Darnley, K. Hornoch, A. V. Filippenko, M. F. Bode, R. Ciardullo, K. A. Misselt, R. A. Hounsell, R. Chornock, and T. Matheson, ApJ **734**, 12 (2011).

M. M. Kasliwal, S. B. Cenko, S. R. Kulkarni, E. O. Ofek, R. Quimby, and A. Rau, ApJ **735**, 94 (2011b).

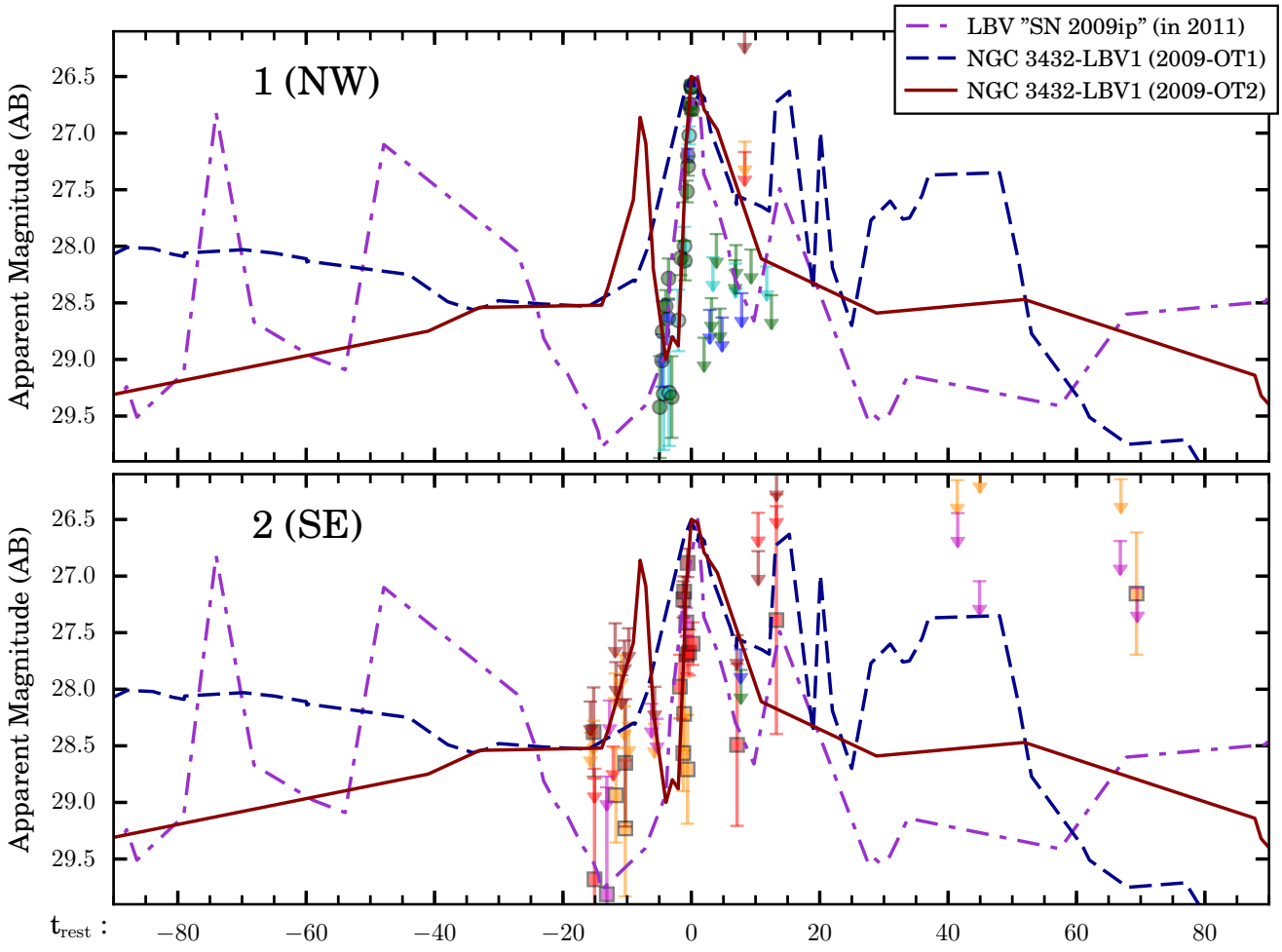

FIG. 11.— Comparison of observed HFF14Spo light curves against rapid outbursts from two LBVs.

I. Hachisu and M. Kato, ApJ **798**, 76 (2015).
R. A. Downes and H. W. Duerbeck, AJ **120**, 2007 (2000).
B. E. Schaefer, ApJS **187**, 275 (2010).
M. J. Darnley, M. Henze, I. A. Steele, M. F. Bode, V. A. R. M. Ribeiro, P. Rodríguez-Gil, A. W. Shafter, S. C. Williams, D. Baer, I. Hachisu, M. Hernanz, K. Hornoch, R. Hounsell, M. Kato, S. Kiyota, H. Kučáková, H. Maehara, J.-U. Ness, A. S. Piascik, G. Sala, I. Skillen, R. J. Smith, and M. Wolf, A&A **580**, A45 (2015).
A. W. Shafter, A. Rau, R. M. Quimby, M. M. Kasliwal, M. F. Bode, M. J. Darnley, and K. A. Misselt, ApJ **690**, 1148 (2009).
I. Czekala, E. Berger, R. Chornock, A. Pastorello, G. H. Marion, R. Margutti, M. T. Botticella, P. Challis, M. Ergon, S. Smartt, J. Sollerman, J. Vinkó, and J. C. Wheeler, ApJ **765**, 57 (2013).
M. della Valle, A&A **252**, L9 (1991).
R. E. Williams, M. M. Phillips, and M. Hamuy, ApJS **90**, 297 (1994).
G. J. Schwarz, S. N. Shore, S. Starrfield, P. H. Hauschildt, M. Della Valle, and E. Baron, MNRAS **320**, 103 (2001).
S. Tang, L. Bildsten, W. M. Wolf, K. L. Li, A. K. H. Kong, Y. Cao, S. B. Cenko, A. De Cia, M. M. Kasliwal, S. R. Kulkarni, R. R. Laher, F. Masci, P. E. Nugent, D. A. Perley, T. A. Prince, and J. Surace, ApJ **786**, 61 (2014).
M. J. Darnley, S. C. Williams, M. F. Bode, M. Henze, J.-U. Ness, A. W. Shafter, K. Hornoch, and V. Votruba, A&A **563**, L9 (2014).
M. Henze, M. J. Darnley, F. Kabashima, K. Nishiyama, K. Itagaki, and X. Gao, A&A **582**, L8 (2015a).
M. Henze, J.-U. Ness, M. J. Darnley, M. F. Bode, S. C. Williams, A. W. Shafter, G. Sala, M. Kato, I. Hachisu, and M. Hernanz, A&A **580**, A46 (2015b).
D. Prialnik and A. Kovetz, ApJ **445**, 789 (1995).
O. Yaron, D. Prialnik, M. M. Shara, and A. Kovetz, ApJ **623**, 398 (2005).
M. Kato, H. Saio, and I. Hachisu, ApJ **808**, 52 (2015).
C. M. Gaskell and E. S. Klimek, Astronomical and Astrophysical Transactions **22**, 661 (2003).
L. A. Balona, MNRAS **423**, 3420 (2012).
C. Karoff, M. F. Knudsen, P. De Cat, A. Bonanno, A. Fogtmann-Schulz, J. Fu, A. Frasca, F. Inceoglu, J. Olsen, Y. Zhang, Y. Hou, Y. Wang, J. Shi, and W. Zhang, Nature Communications **7**, 11058 (2016).
J. Wambsganss, in *Gravitational Lensing: Recent Progress and Future Go*, Astronomical Society of the Pacific Conference Series, Vol. 237, edited by T. G. Brainerd and C. S. Kochanek (2001) p. 185.
C. S. Kochanek, ApJ **605**, 58 (2004).
B. Paczynski, ApJ **304**, 1 (1986).
C. Alcock, C. W. Akerlof, R. A. Allsman, T. S. Axelrod, D. P. Bennett, S. Chan, K. H. Cook, K. C. Freeman, K. Griest, S. L. Marshall, H.-S. Park, S. Perlmutter, B. A. Peterson, M. R. Pratt, P. J. Quinn, A. W. Rodgers, C. W. Stubbs, and W. Sutherland, Nature **365**, 621 (1993).
E. Aubourg, P. Bareyre, S. Bréhin, M. Gros, M. Lachièze-Rey, B. Laurent, E. Lesquoy, C. Magneville, A. Milsztajn, L. Moscoso, F. Queinnec, J. Rich, M. Spiro, L. Vigroux, S. Zylberajch, R. Ansari, F. Cavalier, M. Moniez, J.-P. Beaulieu, R. Ferlet, P. Grison, A. Vidal-Madjar, J. Guibert, O. Moreau, F. Tajahmady, E. Maurice, L. Prévôt, and C. Gry, Nature **365**, 623 (1993).
A. Udalski, M. Szymanski, J. Kaluzny, M. Kubiak, W. Krzeminski, M. Mateo, G. W. Preston, and B. Paczynski, ACTAA **43**, 289 (1993).

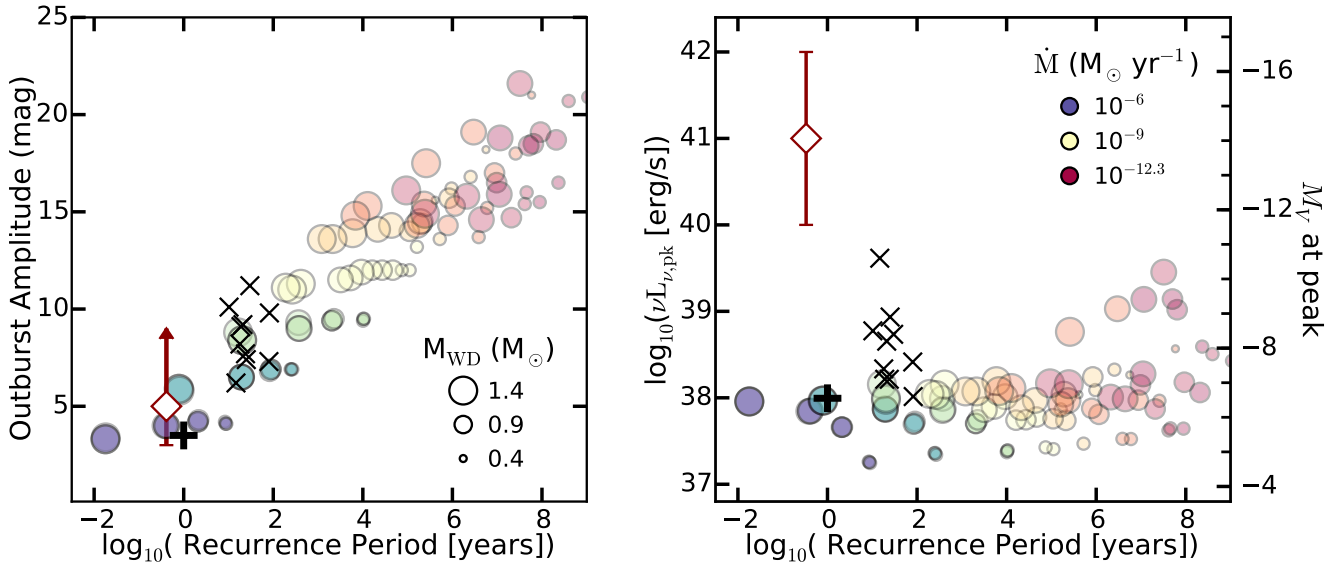

FIG. 12.— Comparison of the inferred HFF14Spo recurrence timescale against observed RNe and models. In the left panel the outburst amplitude in magnitudes is plotted against the recurrence timescale, while in the right panel the y axis shows the peak luminosity (or absolute magnitude). In both panels the joint constraints on HFF14Spo from both transient episodes are plotted as large open diamonds, observed constraints from the 10 galactic RNe appear as black 'x' points, and the rapid-recurrence nova M31N 2008a-12 is shown with a thick black '+' marker. Colored circles show the results from a suite of numerical hydrodynamic simulations from (Yaron *et al.* 2005). The size of each circle indicates the mass of the primary white dwarf (WD) star over the range 0.4-1.4 $M_\odot$, as indicated in the legend of the left panel. The color of each circle denotes the rate of mass transfer from the secondary onto the WD, as given in the right panel's legend.

P. Schneider and A. Weiss, A&A **164**, 237 (1986).

J. MiraldaEscude, ApJ **379**, 94 (1991).

G. F. Lewis, J. Miralda-Escude, D. C. Richardson, and J. Wambsganss, MNRAS **261**, 647 (1993).

K. Chang and S. Refsdal, Nature **282**, 561 (1979).

K. Chang and S. Refsdal, A&A **132**, 168 (1984).

J. Vernet, H. Dekker, S. D'Odorico, L. Kaper, P. Kjaergaard, F. Hammer, S. Randich, F. Zerbi, P. J. Groot, J. Hjorth, I. Guinouard, R. Navarro, T. Adolfse, P. W. Albers, J.-P. Amans, J. J. Andersen, M. I. Andersen, P. Binetruy, P. Bristow, R. Castillo, F. Chemla, L. Christensen, P. Conconi, R. Conzelmann, J. Dam, V. de Caprio, A. de Ugarte Postigo, B. Delabre, P. di Marcantonio, M. Downing, E. Elswijk, G. Finger, G. Fischer, H. Flores, P. François, P. Goldoni, L. Guglielmi, R. Haigron, H. Hanenburg, I. Hendriks, M. Horrobin, D. Horville, N. C. Jessen, F. Kerber, L. Kern, M. Kiekebusch, P. Kleszcz, J. Klougart, J. Kragt, H. H. Larsen, J.-L. Lizon, C. Lucuix, V. Mainieri, R. Manuputy, C. Martayan, E. Mason, R. Mazzoleni, N. Michaelsen, A. Modigliani, S. Moehler, P. Møller, A. Norup Sørensen, P. Nørregaard, C. Péroux, F. Patat, E. Pena, J. Pragt, C. Reinero, F. Rigal, M. Riva, R. Roelfsema, F. Royer, G. Sacco, P. Santin, T. Schoenmaker, P. Spano, E. Sweers, R. Ter Horst, M. Tintori, N. Tromp, P. van Dael, H. van der Vliet, L. Venema, M. Vidali, J. Vinther, P. Vola, R. Winters, D. Wistisen, G. Wulterkens, and A. Zacchei, A&A **536**, A105 (2011).

N. Benítez, ApJ **536**, 571 (2000).

G. B. Brammer, P. G. van Dokkum, and P. Coppi, ApJ **686**, 1503 (2008).

O. Le Fèvre, M. Saisse, D. Mancini, S. Brau-Nogue, O. Caputi, L. Castinel, S. D'Odorico, B. Garilli, M. Kissler-Patig, C. Lucuix, G. Mancini, A. Pauget, G. Sciarretta, M. Scodeggio, L. Tresse, and G. Vettolani, in *Instrument Design and Performance for Optical/Infrared Ground-based Telescopes*, Society of Photo-Optical Instrumentation Engineers (SPIE) Conference Series, Vol. 4841, edited by M. Iye and A. F. M. Moorwood (2003) pp. 1670–1681.

P. Rosati, I. Balestra, C. Grillo, A. Mercurio, M. Nonino, A. Biviano, M. Girardi, E. Vanzella, and Clash-VLT Team, The Messenger **158**, 48 (2014).

C. Grillo, S. H. Suyu, P. Rosati, A. Mercurio, I. Balestra, E. Munari, M. Nonino, G. B. Caminha, M. Lombardi, G. De Lucia, S. Borgani, R. Gobat, A. Biviano, M. Girardi, K. Umetsu, D. Coe, A. M. Koekemoer, M. Postman, A. Zitrin, A. Halkola, T. Broadhurst, B. Sartoris, V. Presotto, M. Annunziatella, C. Maier, A. Fritz, E. Vanzella, and B. Frye, ApJ **800**, 38 (2015).

I. Balestra, A. Mercurio, B. Sartoris, M. Girardi, C. Grillo, M. Nonino, P. Rosati, A. Biviano, S. Ettori, W. Forman, C. Jones, A. Koekemoer, E. Medezinski, G. A. Ogrean, P. Tozzi, K. Umetsu, E. Vanzella, R. J. van Weeren, A. Zitrin, M. Annunziatella, G. B. Caminha, T. Broadhurst, D. Coe, M. Donahue, A. Fritz, B. Frye, D. Kelson, M. Lombardi, C. Maier, M. Meneghetti, A. Monna, M. Postman, M. Scodeggio, S. Seitz, and B. Ziegler, ArXiv e-prints (2015).

F. Henault, R. Bacon, C. Bonneville, D. Boudon, R. L. Davies, P. Ferruit, G. F. Gilmore, O. Le Fèvre, J.-P. Lemonnier, S. Lilly, S. L. Morris, E. Prieto, M. Steinmetz, and P. T. de Zeeuw, in *Instrument Design and Performance for Optical/Infrared Ground-based Telescopes*, Proc. SPIE, Vol. 4841, edited by M. Iye and A. F. M. Moorwood (2003) pp. 1096–1107.

R. Bacon, M. Accardo, L. Adjali, H. Anwand, S.-M. Bauer, J. Blaizot, D. Boudon, J. Brinchmann, L. Brotons, P. Caillier, L. Capoani, M. Carollo, M. Comin, T. Contini, C. Cumani, E. Daguis, S. Deiries, B. Delabre, S. Dreizler, J.-P. Dubois, M. Dupieux, C. Dupuy, E. Emsellem, A. Fleischmann, M. François, G. Gallou, T. Gharsa, N. Girard, A. Glindemann, B. Guiderdoni, T. Hahn, G. Hansali, D. Hofmann, A. Jarno, A. Kelz, M. Kiekebusch, J. Knudstrup, C. Koehler, W. Kollatschny, J. Kosmalski, F. Laurent, M. Le Floch, S. Lilly, J.-L. Lizon à L'Allemand, M. Loupias, A. Manescau, C. Monstein, H. Nicklas, J. Niemeyer, J.-C. Olaya, R. Palsa, L. Parès, L. Pasquini, A. Pécontal-Rousset, R. Pello, C. Petit, L. Piqueras, E. Popow, R. Reiss, A. Remillieux, E. Renault, P. Rhode, J. Richard, J. Roth, G. Rupprecht, J. Schaye, E. Slezak, G. Soucail, M. Steinmetz, O. Streicher, R. Stuik, H. Valentin, J. Vernet, P. Weilbacher, L. Wisotzki, N. Yerle, and G. Zins, The Messenger **147**, 4 (2012).

K. B. Schmidt, T. Treu, G. B. Brammer, M. Bradač, X. Wang, M. Dijkstra, A. Dressler, A. Fontana, R. Gavazzi, A. L. Henry, A. Hoag, T. A. Jones, P. L. Kelly, M. A. Malkan, C. Mason, L. Pentericci, B. Poggianti, M. Stiavelli, M. Trenti, A. von der Linden, and B. Vulcani, ApJ **782**, L36 (2014).

T. Treu, K. B. Schmidt, G. B. Brammer, B. Vulcani, X. Wang, M. Bradač, M. Dijkstra, A. Dressler, A. Fontana, R. Gavazzi, A. L. Henry, A. Hoag, K.-H. Huang, T. A. Jones, P. L. Kelly, M. A. Malkan, C. Mason, L. Pentericci, B. Poggianti, M. Stiavelli, M. Trenti, and A. von der Linden, ApJ **812**, 114 (2015).
D. O. Jones, D. M. Scolnic, and S. A. Rodney, "PythonPhot: Simple DAOPHOT-type photometry in Python," Astrophysics Source Code Library (2015).
D. W. Hogg, I. K. Baldry, M. R. Blanton, and D. J. Eisenstein, ArXiv Astrophysics e-prints (2002).
S. Hemmati, S. H. Miller, B. Mobasher, H. Nayyeri, H. C. Ferguson, Y. Guo, A. M. Koekemoer, D. C. Koo, and C. Papovich, ApJ **797**, 108 (2014).
I. Sendra, J. M. Diego, T. Broadhurst, and R. Lazkoz, MNRAS **437**, 2642 (2014).
M. Jauzac, B. Clément, M. Limousin, J. Richard, E. Jullo, H. Ebeling, H. Atek, J.-P. Kneib, K. Knowles, P. Natarajan, D. Eckert, E. Egami, R. Massey, and M. Rexroth, MNRAS **443**, 1549 (2014).
E. Jullo, J.-P. Kneib, M. Limousin, Á. Elíasdóttir, P. J. Marshall, and T. Verdugo, New Journal of Physics **9**, 447 (2007).
J. F. Navarro, C. S. Frenk, and S. D. M. White, ApJ **490**, 493 (1997).
R. Kawamata, M. Oguri, M. Ishigaki, K. Shimasaku, and M. Ouchi, ArXiv e-prints, arXiv:1510.06400 (2015).
J. Liesenborgs, S. De Rijcke, and H. Dejonghe, MNRAS **367**, 1209 (2006).
J. Liesenborgs, S. de Rijcke, H. Dejonghe, and P. Bekaert, MNRAS **380**, 1729 (2007).
I. Mohammed, J. Liesenborgs, P. Saha, and L. L. R. Williams, MNRAS **439**, 2651 (2014).
H. C. Plummer, MNRAS **71**, 460 (1911).
A. Zitrin, T. Broadhurst, K. Umetsu, D. Coe, N. Benítez, B. Ascaso, L. Bradley, H. Ford, J. Jee, E. Medezinski, Y. Rephaeli, and W. Zheng, MNRAS **396**, 1985 (2009).
M. Postman, D. Coe, N. Benítez, L. Bradley, T. Broadhurst, M. Donahue, H. Ford, O. Graur, G. Graves, S. Jouvel, A. Koekemoer, D. Lemze, E. Medezinski, A. Molino, L. Moustakas, S. Ogaz, A. Riess, S. Rodney, P. Rosati, K. Umetsu, W. Zheng, A. Zitrin, M. Bartelmann, R. Bouwens, N. Czakon, S. Golwala, O. Host, L. Infante, S. Jha, Y. Jimenez-Teja, D. Kelson, O. Lahav, R. Lazkoz, D. Maoz, C. McCully, P. Melchior, M. Meneghetti, J. Merten, J. Moustakas, M. Nonino, B. Patel, E. Regös, J. Sayers, S. Seitz, and A. Van der Wel, ApJS **199**, 25 (2012).
A. W. Mann and H. Ebeling, MNRAS **420**, 2120 (2012).
L. Christensen, J. Richard, J. Hjorth, B. Milvang-Jensen, P. Laursen, M. Limousin, M. Dessauges-Zavadsky, C. Grillo, and H. Ebeling, MNRAS **427**, 1953 (2012).
J. Priewe, L. L. R. Williams, J. Liesenborgs, D. Coe, and S. A. Rodney, ArXiv e-prints (2016)